Emma Jakab

Analytical Techniques as a Tool to Understand the Reaction Mechanism

Chapter 3

in

Recent Advances in Thermo-chemical Conversion of Biomass

Editors: A. Pandey, T. Bhaskar, M. Stocker &

R. K. Sukumaran

Elsevier, 2015, pp. 73-106.

http://dx.doi.org/10.1016/B978-0-444-63289-0.00003-X

Chapter 3

Analytical Techniques as a Tool to Understand the Reaction Mechanism

Emma Jakab

Institute of Materials and Environmental Chemistry, Research Center for Natural Sciences, Hungarian Academy of Sciences, Magyar Tudósok krt. 2, Budapest, H-1117 Hungary
E-mail: jakab.emma@ttk.mta.hu

Contents

ABSTRACT

Thermal decomposition of biomass samples and the major macromolecular constituents of lignocellulosic biomass are reviewed. Special emphasis has been placed on the results of the thermoanalytical methods and analytical pyrolysis. On the basis of the product distribution of the thermal decomposition, the possible major decomposition mechanisms are discussed. The influence of the inherent inorganic components of biomass on the thermal decomposition of cellulose, and lignin are demonstrated. Furthermore, the effect of the low temperature heat treatment, the torrefaction on the thermal conversions are summarized.

Keywords: Biomass; Thermogravimetry; Analytical Pyrolysis; Gas chromatography/mass spectrometry; Cellulose; Lignin; Hemicellulose; Mechanism.

3.1. INTRODUCTION

Biomass, as a renewable energy source, can either be used directly via combustion to produce heat, or indirectly by converting it to various biofuels by thermal conversion processes. Depending on the conditions of thermal treatment, pyrolysis, torrefaction, gasification, hydrothermal treatment are the most frequently used techniques. In order to produce various chemicals from biomass by thermal conversion methods, the composition of biomass and the thermal decomposition mechanisms should be determined.

Biomass is a complex material which contains several natural polymers, extractable materials and inorganic compounds. In this chapter, we discuss the thermal decomposition of lignocellulosic biomass samples, since they are preferred for energetic utilization. We do not deal with the protein-containing biomass, which are primarily used for food. Biomass samples are not soluble in conventional solvents therefore they cannot be studied by most of the conventional analytical techniques. Nevertheless, degradative methods can be used for the characterization of the composition and structure of biomass samples. For this purpose analytical techniques can be used, where small amount of samples are applied and therefore the probability of the secondary reactions are minimized. The analytical thermal methods can be classified into thermal analysis methods and pyrolytic techniques.

Thermal analysis includes those thermal methods where certain physical properties of the materials are measured as they change with temperature or time. Several methods are commonly employed depending on the property which is measured. The most frequently used thermoanalytical techniques are the following: thermogravimetry where the mass is monitored, differential scanning calorimetry where the heat loss or heat consumption is measured and thermomechanical analysis where the dimension of the samples are observed. The thermoanalytical methods apply relatively low heating rates and the physical properties of the samples are monitored as a function of temperature or time. The applied atmosphere can be either inert or oxidative, even vacuum can be used in certain thermobalances.

The analytical pyrolysis refers to a thermal decomposition method, where the samples are heated usually fast to a given temperature in inert atmosphere. Generally thermal decomposition products of organic materials are studied using flash pyrolysis. Some of the pyrolysis products are not stable therefore the analytical pyrolyzers are coupled on-line to a

gas chromatograph (GC) or mass spectrometer (MS) to monitor the primary decomposition products. Nowadays the pyrolyzers are most commonly used with a GC/MS system, where the GC instrument separates the pyrolysis products and the qualitative and quantitative determinations of the individual products are carried out by the mass spectrometer.

3.2. COMPOSITION OF LIGNOCELLULOSIC BIOMASS SAMPLES

As it is well-known, cellulose, hemicellulose and lignin are the major natural polymeric components of the biomass samples [1]. Cellulose is a linear macromolecule of high molecular mass, which is composed of D-glucopyranose units linked with β-(1-4)-O-bonds. Aggregation of cellulose chains within the microfibrils provides a crystalline structure. Cellulose microfibrils are embedded in a matrix of hemicelluloses and lignin forming the main components of the cell walls and lignocellulosic biomass in general.

The nature of hemicellulose and lignin varies with the type of biomass. O-acetyl-4-O-methylglucuronoxylan forms the main hemicellulose of the hardwoods. Hemicelluloses in softwoods are mainly galactoglucomannan, containing mannose/glucose/galactose residues in a ratio of 3/1/1, and glucomannan with mannose/glucose residues in a ratio of 3/1. In herbaceous biomass, arabinoxylans are the predominant hemicellulose polysaccharides. Hemicelluloses are amorphous, have a lower degree of polymerization than cellulose.

Lignin is a randomly linked, amorphous, cross-linked polymer of phenolic monomers. The softwood lignin contains guaiacyl propane units; hardwood lignin, in addition to this, contains syringyl propane units. The lignin of herbaceous plants contains hydroxyphenylpropane units, too.

Table 3.1 compares the chemical composition of a few biomass species [2]. Wood samples have high cellulose content and low ash content. Hardwoods contain more hemicelluloses and less lignin than softwoods. The composition of herbaceous plants varies in the amounts of macromolecular units, extractable materials and the inorganic content, too.

3.3. THERMAL ANALYSIS

3.3.1. Reaction Heat of the Biomass Decomposition

Thermogravimetric analysis is the most frequently applied thermoanalytical method for the thermal decomposition studies of biomass. A growing number of investigations have applied differential scanning calorimetry (DSC) and differential thermal analysis (DTA) for measuring the reaction heat of the decomposition due to the availability of combined TGA/DSC or TGA/DTA instruments. The thermal decompositions of cellulose [3] and hemicellulose [4] in inert atmosphere are endothermic reactions. Statheropoulos *et al*. [4] studied the thermal decomposition of pine needles by DSC and established that endotherm peaks could be attributed to the desorption of high volatility compounds, moisture, softening and/or melting of the waxy constituents of pine-needles; as well as to the degradation of hemicellulose and cellulose. Exotherm peaks could be attributed to the pyrolysis of lignin and char recombination. Faix *et al*. [5] studied the decomposition of milled wood lignins in inert atmosphere and exotherm reactions were also observed in the 200-400°C temperature range.

Table 3.1. Proximate analysis of some biomass species. Data are taken from ref. 2 with the permission of Elsevier.

Species	Total ash (%)	Solvent soluble (%)	Water soluble (%)	Lignin (%)	Hemicellulose (%)	Cellulose (%)
Softwood	0.4	2.0	-	27.8	24.0	41.0
Hardwood	0.3	3.1	-	19.5	35.0	39.0
Wheat straw	6.6	3.7	7.4	16.7	28.2	39.9
Rice straw	16.1	4.6	13.3	11.9	24.5	30.2
Bagasse	1.6	0.3	-	20.2	38.5	38.1

3.3.2. Thermogravimetric Analysis of Biomass

Thermogravimetric analysis (TGA) provides a mass change profile as a function of the sample temperature or analysis time, thus the thermal decomposition processes can be monitored. The TGA curves and the derivative thermogravimetric curves (DTG) give information about the thermal stability of the sample and the overall kinetic progress of the thermal decomposition. The thermal decomposition studies of biomass samples started several decades ago. Among the early publications, the pioneering work of F. Shafizadeh and his coworkers must be mentioned [2, 3, 6, 7]. They applied thermogravimetry and furnace pyrolysis and analyzed the volatile products off-line by various analytical techniques. The mechanisms of the primary and secondary reactions of thermal decomposition and combustion of cellulosic materials have been established [2, 6].

Fig. 3.1 shows the instrumental setup of the thermogravimetric system used for the analyses of biomass samples described in this chapter. About 2-4 mg samples were placed into the platinum sample pan and the furnace was flushed with the carrier gas thoroughly before the experiments. Generally 10°C/min or 20°C/min linear heating rate was applied. For thermal decomposition studies argon was used as a flushing gas. The volatile decomposition products were analyzed on-line by a mass spectrometer.

Fig. 3.2 presents the thermogravimetric curves of the three major macromolecular components of biomass in inert atmosphere. Avicel PH-105 is a microcrystalline cellulose representing similar crystalline structure as the biomass samples have (α-cellulose) [1] . O-acetyl-4-O-methyl-D-glucurono-xylan is a typical hardwood xylan, which was isolated from beech wood [8]. Milled wood lignin was also isolated from beech wood according to Björkman procedure [9]. As the DTG curves show, the carbohydrates decompose with a high decomposition rate in a rather small temperature interval. Cellulose produces a sharp DTG

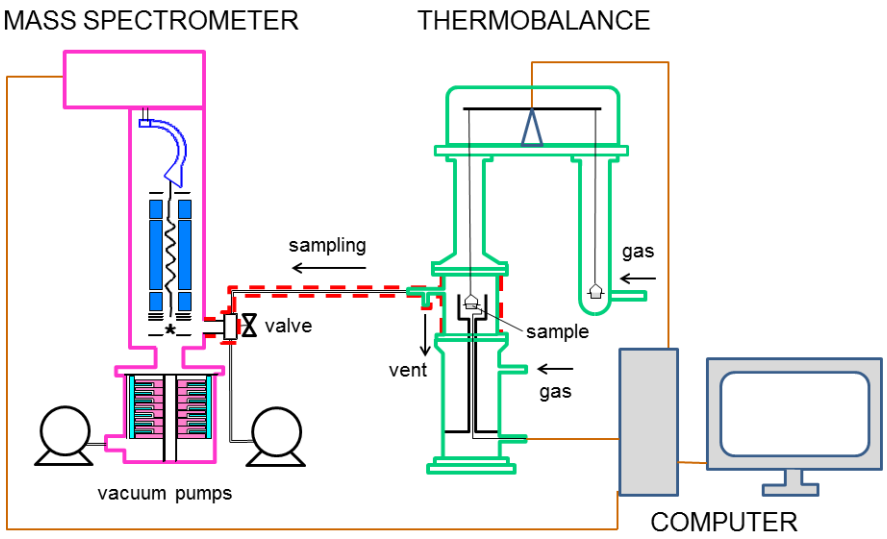

Figure 3.1. Thermogravimetry/mass spectrometry instrument. The thermobalance applied is a modified Perkin-Elmer TGS-2, while the mass spectrometer is a Hiden HAL 2/PIC instrument.

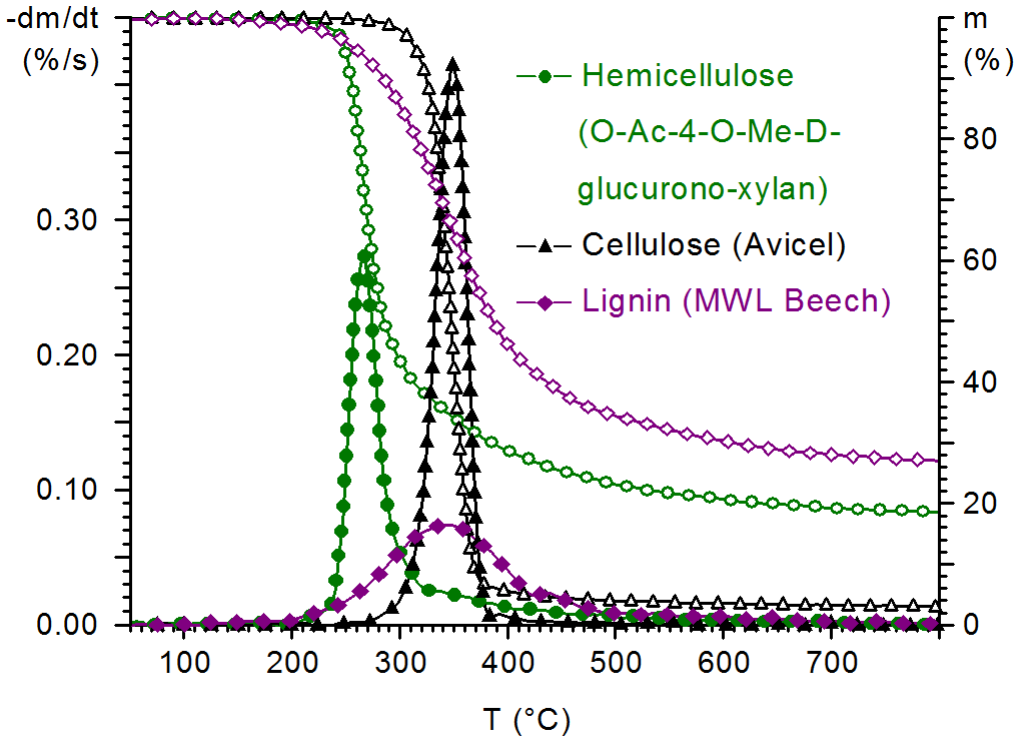

Figure 3.2. Thermogravimetric curves of wood components in argon atmosphere using 10°C/min heating rate and 2-3 mg sample sizes. Open symbols, TGA curves; Closed symbols, DTG curves.

peak and small amount of char residue. The xylan polymer decomposes at a lower temperature, which can be explained by the presence of thermolabile functional groups

(acetyl groups), the amorphous structure and lower molecular mass. Lignin decomposes in a wide temperature range with a small decomposition rate and produces about 30% char residue due to its cross-linked aromatic structure.

Fig. 3.3 illustrates the TG and DTG curves calculated from the curves of the 3 components in the ratio of hemicellulose:cellulose:lignin=0.333:0.394:0.248 based on the composition of beech wood [1]. The extractive and inorganic contents were not taken into account. The thermogravimetric curves of beech wood sample differs significantly from the sum of the TG and DTG curves of the components, although the char yields are quite similar. The most considerable difference is that the decomposition of hemicellulose and the cellulose is not separated well and only a shoulder on the DTG curve indicates the presence of hemicellulose decomposition. Several reasons may explain the differences. The biomass samples contain inorganic compounds, which have strong influence on the decomposition mechanisms [10, 11] as will be discussed later. Furthermore, covalent chemical bonds exist between the macromolecules in the biomass [12], which might affect the thermal stability. The physical and chemical structure of the isolated components may differ from their original structure in the biomass, the molecular mass of the isolated compounds are probably smaller than the original one.

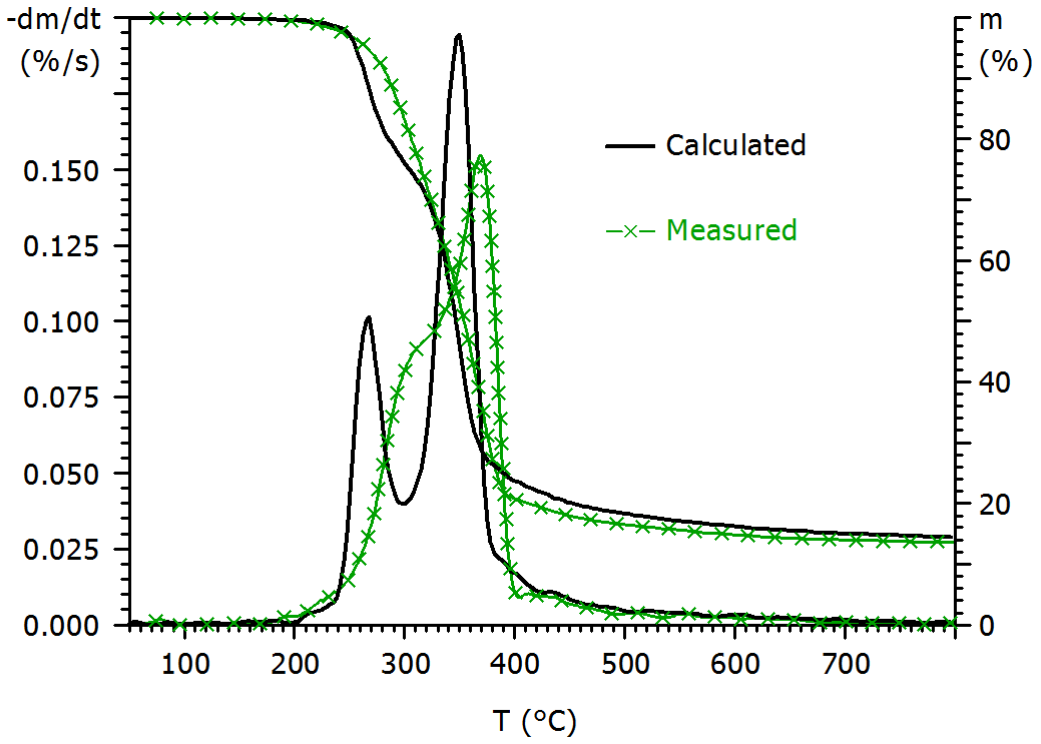

Figure 3.3. Calculated and measured thermogravimetric curves of beech wood using 10°C/min heating rate in argon atmosphere. The curve was calculated from the measured components' curves (Fig.2). The amount of extracts and the inorganic content were neglected.

Table 3.2. Thermogravimetric parameters of biomass samples. The samples were measured in a modified Perkin-Elmer TGS-2 thermobalance at a 20°C/min heating rate in argon atmosphere using 2-4 mg sample sizes.

Sample	T_{start} (extrapol) (°C)	$T_{start(1\%)}$ (°C)	T_{max} (°C)	$T_{end(cel)}$ (°C)	DTG_{max} (%/s)	Char yield (%)
Avicel cellulose	300	290	352	382	0.755	4.1
Whatman cellulose	330	300	379	410	0.708	6.4
Hemicellulose (xylan)	230	221	272	320	0.487	19
Cotton wool	325	277	379	408	0.661	8.3
Flax fiber	240	260	371	400	0.641	10.5
Hemp	220	252	365	397	0.582	12.8
Wheat straw	190	213	328	368	0.303	26.0
Rape straw	190	199	333	376	0.253	13.7
Eucalypt (wood and leaves)	180	207	352	378	0.203	22.8
Olive tree (wood and leaves)	170	161	350	398	0.170	22.4
Pine	240	218	379	413	0.306	16.1
Birch	250	237	392	422	0.321	10.3
Willow	190	207	377	408	0.272	16.8
Poplar	190	210	370	402	0.281	17.3
Black locust	190	195	369	403	0.281	16.7
Beech wood	250	247	381	411	0.349	13.4
MWL Beech	210	229	364	(560)	0.146	27.2
MWL Spruce	190	198	416	(590)	0.109	35.6

Table 3.2 summarizes the major thermogravimetric parameters of several biomass samples as well as cellulose, hemicellulose and lignin. The explanation of the used parameters is illustrated in Fig. 3.4. Two temperatures are used for the characterization of the beginning of the thermal decomposition: $T_{1\%}$ marks the temperature belonging to 1% weight loss of the dry sample (from 150°C), T_{hc} denotes the extrapolated temperature of the beginning of decomposition. The two temperature values can be quite different if the sample contains large amounts of extractable materials, which generally starts to evaporate at lower temperatures with low mass loss rate. T_c stands for the extrapolated temperature of the end of cellulose decomposition in case of the cellulosic samples; it denotes the extrapolated temperature of the end of lignin decomposition in the milled wood lignin (MWL) samples. T_{peak} denotes the temperature of the maximal decomposition rate (DTG_{max}).

Table 3.2 shows the thermogravimetric parameters of two cellulose samples. Whatman cellulose is manufactured from cotton linters having α-cellulose content above 98%. Avicel

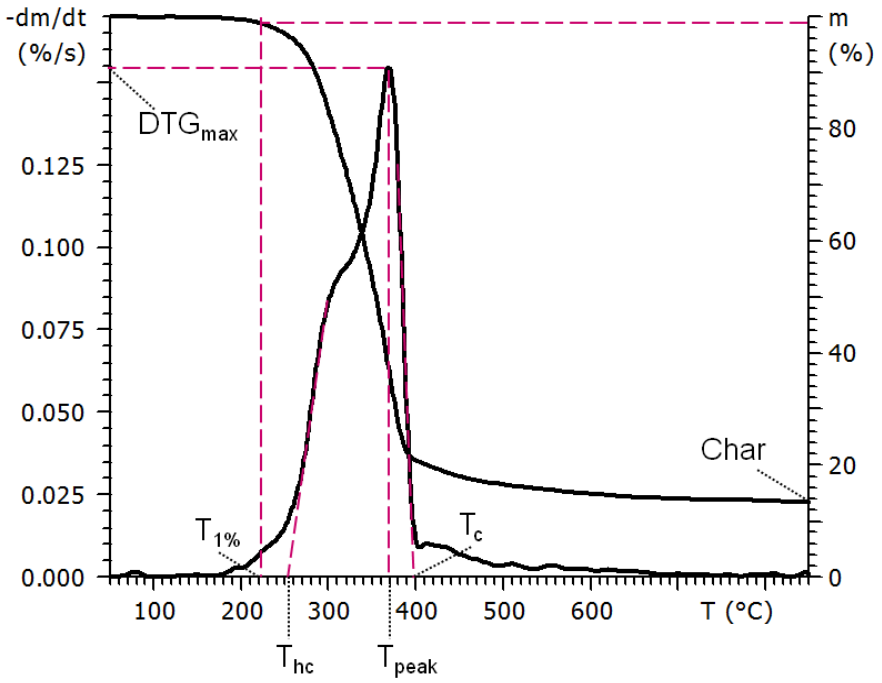

Figure 3.4. The most important thermogravimetric parameters used for biomass samples in Table 3.2.

is a microcrystalline α-cellulose, but its molecular mass is smaller due to the partial acidic hydrolysis during the cleaning process. Apparently the lower molecular mass explains the lower thermal stability of Avicel cellulose. Cotton wool has similar thermal behavior as Whatman cellulose owing to their similar origin. Flax and hemp start to decompose at a lower temperature due to their hemicellulose content, but the maximal rate of decomposition is similar to cotton. The decomposition of the cellulose component in the wood samples takes place rather similarly with the maximal rate of decomposition occurring between 370 and 390°C. The wood samples produce about 10-17% char residue, which can be explained partly by the presence of lignin, partly by the enhancement of charring of carbohydrates in the presence of inorganic components. The whole biomass samples produced even higher char yields. For example, the samples that contained tree branches with bark and leaves (eucalypt and olive tree) had char yields near 22%. The char yield of the herbaceous plants varies in a wide range which can be explained by the catalytic effect of the different inorganic content as will be discussed later. The biomass samples start to decompose at various temperatures due to their different extractive components. Eucalypt and olive tree samples begin to decompose at the lowest temperature because their oil content evaporates already above 150°C.

3.3.3. Thermal Decomposition Products as Measured by Thermogravimetry/Mass spectrometry

The volatile products of the thermal decomposition can be analyzed by several techniques. In earlier biomass literature the decomposition products were analyzed off-line by various methods, e.g., GC, IR, NMR, MS [10, 13]. However, some of the volatile products of

biomass decomposition are not stable, and secondary reactions may occur during the off-line analysis. Coupled techniques provide immediate monitoring of the volatile products released during the thermogravimetric experiments. Thermogravimetry/mass spectrometry (TG/MS) [5, 14] and TG/FTIR [15] represent the most frequently applied coupled techniques in thermal analysis. Fig. 3.1. presents the TG/MS system used for monitoring the evolution of low molecular mass products during the thermogravimetric experiment. A portion of the volatile products was introduced into the ion source of the mass spectrometer through a heated glass-lined metal capillary and a valve. The quadrupole MS operated in electron impact mode at a 70 eV electron energy.

Fig. 3.5. illustrates the thermogravimetric curves and the mass spectrometric evolution profiles of the main detected decomposition products of a hard wood and a herbaceous plant. Panels a and b show the evolution of the main permanent gases and water in the same scales from black locust wood and wheat straw. More gaseous products and water are released from the herbaceous plant than from the wood sample. On the other hand, wheat straw produces 26% char residue including 5% ash, while black locust yields 14% char with only 0.5% ash. Wheat straw has 1.7%, whereas black locust contains only 0.1% potassium. As will be discussed later, the presence of K-ions promotes the formation of char and gaseous products. Furthermore, the decomposition of cellulose is shifted to lower temperatures due to the catalytic effect of K ions. Therefore the maximal rate of decomposition of wheat straw is at 328°C, while it is at 369°C in case of black locust (Table 3.2). The thermal decomposition of hemicellulose is less influenced by the presence of inorganics, thus it is not separated well from the cellulose decomposition, when the cellulose decomposition is shifted to significantly lower temperature.

As Fig. 3.5 a-b shows, some adsorbed water is released at about 100°C from the dried samples, but the majority of water is evolved during the major decomposition range. The carbohydrates and lignin contain various types of hydroxyl groups which may be released as water during heating. Similarly, carbon monoxide and carbon dioxide may be formed from the oxygen-containing functional groups. Methane produces a broad double peak at higher temperatures. The first methane peak at around 430°C can be attributed to the lignin decomposition, it may be derived from the methoxyl groups of lignin [16]. Black locust as a hard wood has more methoxyl groups as the herbaceous wheat straw, so the wood evolves more methane at lower temperature. However, the charring reactions are more pronounced in the wheat straw, therefore it produces higher methane peak from 450 to 700°C. The final charring process ends with the development of hydrogen from 550 to 900°C.

Fig. 3.5 c-d presents the formation of a few fragment ions and two molecular ions. Formaldehyde can be formed from each macromolecular component of biomass. The molecular ion at *m/z* 60 represents acetic acid at lower temperature (about 300°C), which is released from the side groups of hemicellulose. However, *m/z* 60 can also be attributed to hydroxyacetaldehyde, which is released from cellulose at somewhat higher temperature. Methoxyl ions (m/z 31) can be formed in the mass spectrometer from hydroxyacetaldehyde and from methanol. A typical fragment ion of aldehydes and ketones is m/z 43, which is mostly released from cellulose. Hydrocarbon fragments can also be detected, they are also formed at higher temperature, where lignin decomposition and the charring process occur.

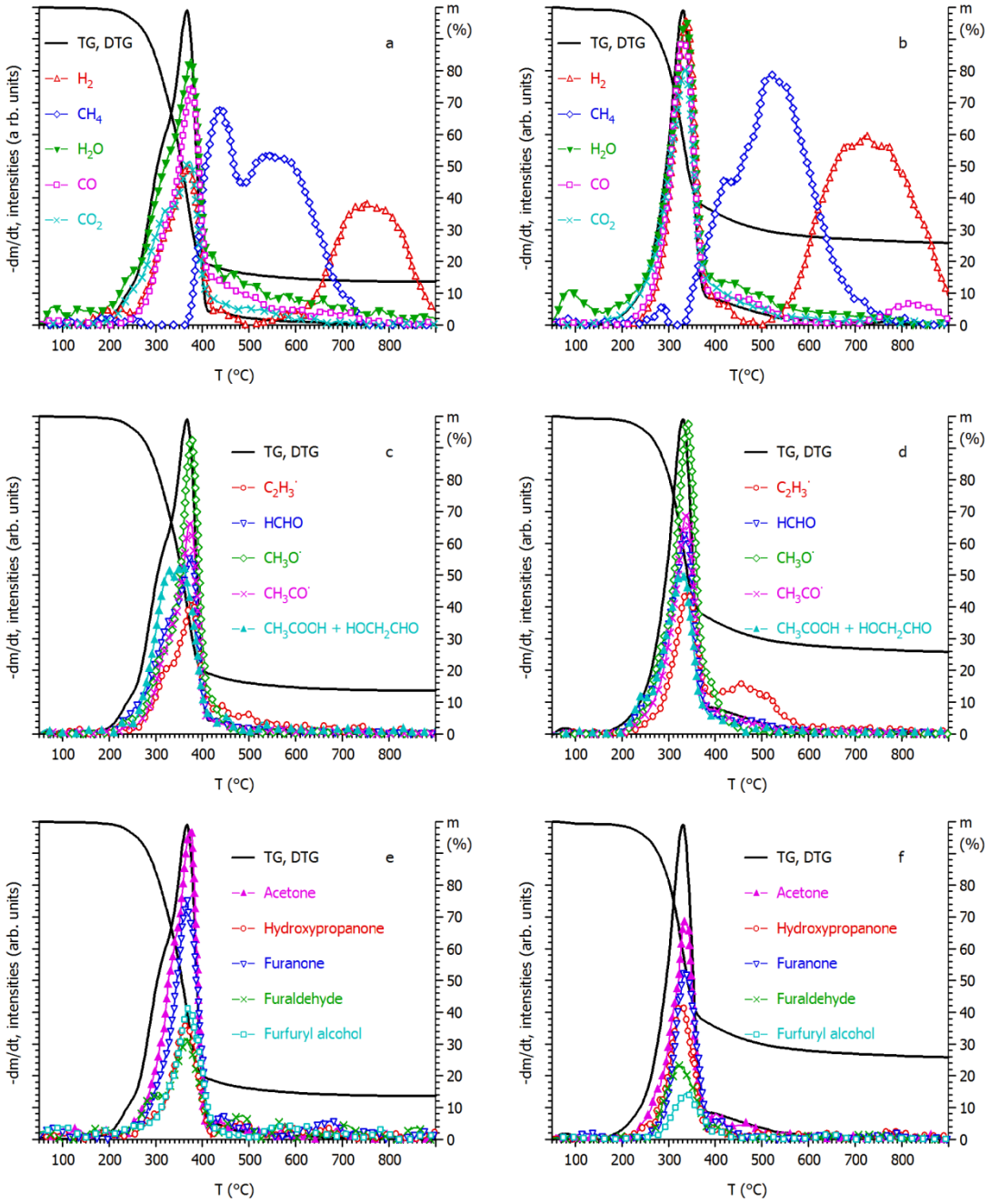

Figure 3.5. Thermogravimetric and mass spectrometric evolution curves during TG/MS experiment of black locust (a, c, e) and wheat straw (b, d, f) in argon atmosphere using 20°C/min heating rate and 3-4 mg sample sizes. The following MS signals were plotted: (a, b) *m/z* 2, 16, 18, 28, 44; (c, d) *m/z* 27, 30, 31, 43, 60; (e, f) *m/z* 58, 74, 84, 96, 98.

Fig. 3.5 e-f shows the evolution of a few oxo- and furan compounds. As it is well-known, the pyranose ring of carbohydrates can be transformed to furanose ring, thus furan-derivatives are typical decomposition products of carbohydrates. These are mostly formed from cellulose, but furanaldehyde is also released from hemicellulose in a significant amount.

The yields of these higher molecular mass compounds are higher during the decomposition of wood than from wheat straw. It should be noted that levoglucosan is a characteristic decomposition product of cellulose, and phenol derivatives are released during the thermal decomposition of lignin. However, they could not be detected by TG/MS because they were condensed in the transfer line between the TGA furnace and the MS due to their polarity and higher molecular mass. Nevertheless, these polar compounds can be monitored by on-line pyrolysis-gas chromatography.

3.3.4. Reaction Kinetic Modeling Using Thermogravimetric Data

The thermogravimetric curves show the rates of weight loss during the thermal decomposition of biomass samples, therefore they are related to the kinetics of these reactions. The first kinetic calculations were made on the TG curves measured at various isothermal temperatures. Generally first order kinetics were assumed, and an Arrhenius plot was used for calculating the activation energy, where the log of the normalized weight was plotted against time [6, 17]. In isothermal experiments, a considerable fraction of the sample may decompose while warming up to the required temperature and this may bias the results. Therefore it is more straightforward to use dynamic conditions. For the determination of the kinetics parameters, the knowledge of the reaction mechanism is crucial. However, even the thermal decomposition of cellulose occurs through several independent reactions. Kilzer and Broido [18] stated that the pyrolysis of cellulose involves three groups of processes: intramolecular dehydration to form anhydrocelluloses, depolymerization leading to levoglucosan evolution, fragmentation reactions producing gases and volatile compounds. It should be emphasized that each partial reaction may be the average of several parallel reactions. In spite of the complicated reaction mechanisms of the thermal decomposition of cellulose, generally first order kinetics are used for modeling indicating that one of the reactions of the complex reaction network is rate controlling. The least squares evaluation method is applied in the most sophisticated models, which generally results in activation energy E=200-240 kJ/mol and preexponential factor $A=10^{15}$-10^{17} s^{-1} for cellulose decomposition [19-22]. However, much lower activation energies have also been reported (e.g., 140-150 kJ/mol) [23]. Várhegyi *et al*. emphasized [19] that low sample masses should be used (0.3-0.5mg) to avoid the heat transfer problems and minimize the secondary reactions during the diffusion of the volatile products.

Fewer kinetics calculations have been carried out on the thermal decomposition of hemicelluloses than on cellulose pyrolysis due to the difficult isolation of hemicelluloses. A few studies are available concerning the chemical kinetics and products of pyrolysis of xylan [24-26], used as a model compound for hardwood hemicelluloses. However, the acetyl groups are split from the O-acetyl-4-O-methylglucoronoxylan molecules during the most frequently used isolation methods. Since the acetyl groups significantly modify the thermal stability of the molecules, the kinetic studies on xylan macromolecules do not represent completely the thermal decomposition of hardwood hemicelluloses. Di Blasi [26] obtained activation energies of 76 kJ/mol for volatile evolution and of 114-143 kJ/mol for char formation during isothermal pyrolysis of xylan. Várhegyi *et al*. [25] applied a successive reaction model for nonisothermal thermogravimetric experiments of xylan resulting in about

195 kJ/mol and 95 kJ/mol activation energy for the two reaction steps. Branca *et al*. [27] studied the pyrolysis kinetics of glucomannan, the main component of softwood hemicelluloses. Isothermal kinetics were applied for the yield of volatile products and char, and activation energies between 52 and 96 kJ/mol were obtained.

The kinetic description of lignin is more difficult than that of cellulose. Lignin decomposes in a wide temperature range with a low decomposition rate producing a wide and flat DTG curve. The cross-linked nature of lignin structure and the different thermal stability of the various functional groups lead to very diverse reactions. Therefore, the corresponding reaction mechanisms are too complex for the mathematical modeling. Várhegyi *et al*. [19] described the thermal decomposition of milled wood lignins by a formal approximation using a pseudo first order reaction and received extremely low activation energies of 34-65 kJ/mol.

Numerous kinetic calculations can be found in the literature for the thermogravimetric experiments of biomass samples with very diverse results [28-34]. The kinetic models generally assume that the isothermal gas or liquid phase models can be applied for the dynamic experiments. Due to the complex composition of biomass materials, the TGA experiments of biomass materials are evaluated nowadays by the nonlinear method of least-squares (LSQ), assuming more than one reaction. Lignocellulosic materials consist of three main macromolecular components: hemicellulose, cellulose and lignin. It is frequently supposed in the kinetic models that the thermal decomposition of the biomass components takes place independently from each other. The three-component mechanism with linear or nonlinear dependence on the species concentrations, for the volatile fractions of the pseudo-components hemicellulose, cellulose and lignin, is widely applied [28-33] to describe the dynamic thermogravimetric curves of wood/biomass devolatilization. The first pseudo-component is associated with the shoulder and the second one with the peak of the DTG curve, whereas the lignin pseudo-component decomposes slowly over a very broad range of temperatures. The calculated activation energies vary between 80 and 116 kJ/mol for hemicellulose, 195–286 kJ/mol for cellulose, and 18–65 kJ/mol for lignin. Nevertheless, Caballero *et al*. [35] concluded that some interactions must exist between the biomass components during the thermal decompositions because the simple addition of the kinetics of isolated compounds (hemicellulose, cellulose, lignin) cannot satisfactorily reproduce the kinetic behavior of the raw materials. Furthermore, the additive models are not able to explain the fact that higher heating rates result in the formation of less char from biomass samples.

The assumption of a distribution of the reactivity of species frequently helps in the kinetic evaluation of the pyrolysis of complex organic samples. The distributed activation energy models (DAEM) have also been used for biomass kinetics [36-38]. The thermal decomposition has been described by three partial reactions assuming Gaussian distribution for the activation energies.

The thermal decomposition of large particles of lignocellulosic fuels is interesting from the viewpoint of thermochemical conversion processes. Di Blasi *et al*. [39, 40] studied the effect of transport phenomena and heat radiation intensity on the process dynamics, macroscopic behavior, conversion, pyrolysis product yields of various biomass samples. This study provided fundamental information for reactor optimization when internal heat transfer is the controlling mechanism.

3.4. ANALYTICAL PYROLYSIS

3.4.1. Pyrolysis Techniques

The principle of flash pyrolysis is the fast heating to a predetermined temperature and keeping the sample at the constant temperature for a given time. The pyrolysis is carried out in inert atmosphere, helium is used most frequently especially with mass spectrometric detections. The rapid heating of solid samples can be carried out by different techniques [41-43]. The furnace-type pyrolyzer is heated to the given temperature continuously and the sample is introduced into the preheated zone rapidly. The resistively heated metal element utilizes mostly a coiled platinum filament with a quartz tube for solid samples or a platinum ribbon for soluble samples. Curie-point pyrolysis applies high frequency inductive heating of ferromagnetic wires or small sheets. The samples are placed on the wires from suspension or packed in the sheets, and they are pyrolyzed at the Curie temperature of the ferromagnetic alloys. Laser pyrolysis is used when vigorous degradation of the samples is necessary, but only small surface of the sample can be reached by the laser light.

The volatile products of the pyrolysis usually are measured on-line by an analytical instrument. Two kinds of techniques are commonly applied. The pyrolysis unit can be coupled to a mass spectrometer or a Fourier transform infrared spectrometer, which monitor the spectra and the intensity of all the products. These procedures are very fast and suitable for fingerprinting studies and statistical pattern recognition methods of large number of samples. The other widely applied technique use the coupling of the pyrolysis unit with a gas chromatograph, which separates the volatile products. The detector can be a regular GC detector (e.g., flame ionization detector), an FTIR equipment or a mass spectrometer. These techniques are more time-consuming, but give a more detailed information about the individual compounds of the pyrolyzate.

3.4.2. Pyrolysis of Macromolecular Biomass Constituents

Formation of levoglucosan (1,6-anhydro-β-D-glucopyranose) during vacuum pyrolysis of cotton cellulose was already reported in 1918 by Pictet and Sarasin [44]. The yield of levoglucosan and other products strongly depends on the purity and physical properties of cellulose as well as on the conditions of pyrolysis. Vacuum pyrolysis can lead to as high as 40-60% levoglucosan yield [2, 45]. Recently Kwon *et al*. [46] reported even 70% levoglucosan yield in a continuous-feed pyrolyzer at 450°C with rapid cooling under reduced pressure of air. According to Mamleev *et al*. [47], the optimal temperature for the production of maximum yield of levoglucosan is 310-340°C. Apparently this temperature is in agreement with the thermogravimetric results on cellulose decomposition [48]. The reaction rate of cellulose decomposition was shown to be inversely proportional to the degree of polymerization and related to the orientation and crystallinity during thermal decomposition in vacuum [49-51]. Levoglucosan appears to be produced from the less ordered regions.

It was shown by Golova *et al*. [52] that 1,6-anhydroglucofuranose is also formed in the thermal decomposition of cellulose under vacuum, the yield being 3% based on cellulose. It has been concluded by Madorsky *et al*. [17] that the pyrolysis of cellulose in nitrogen

atmosphere proceeds at a similar rate as under vacuum, but the product distribution is different: lower amount of tar and greater yield of the lighter fractions are formed under atmospheric pressure, which was explained by secondary reactions of the intermediate fragments.

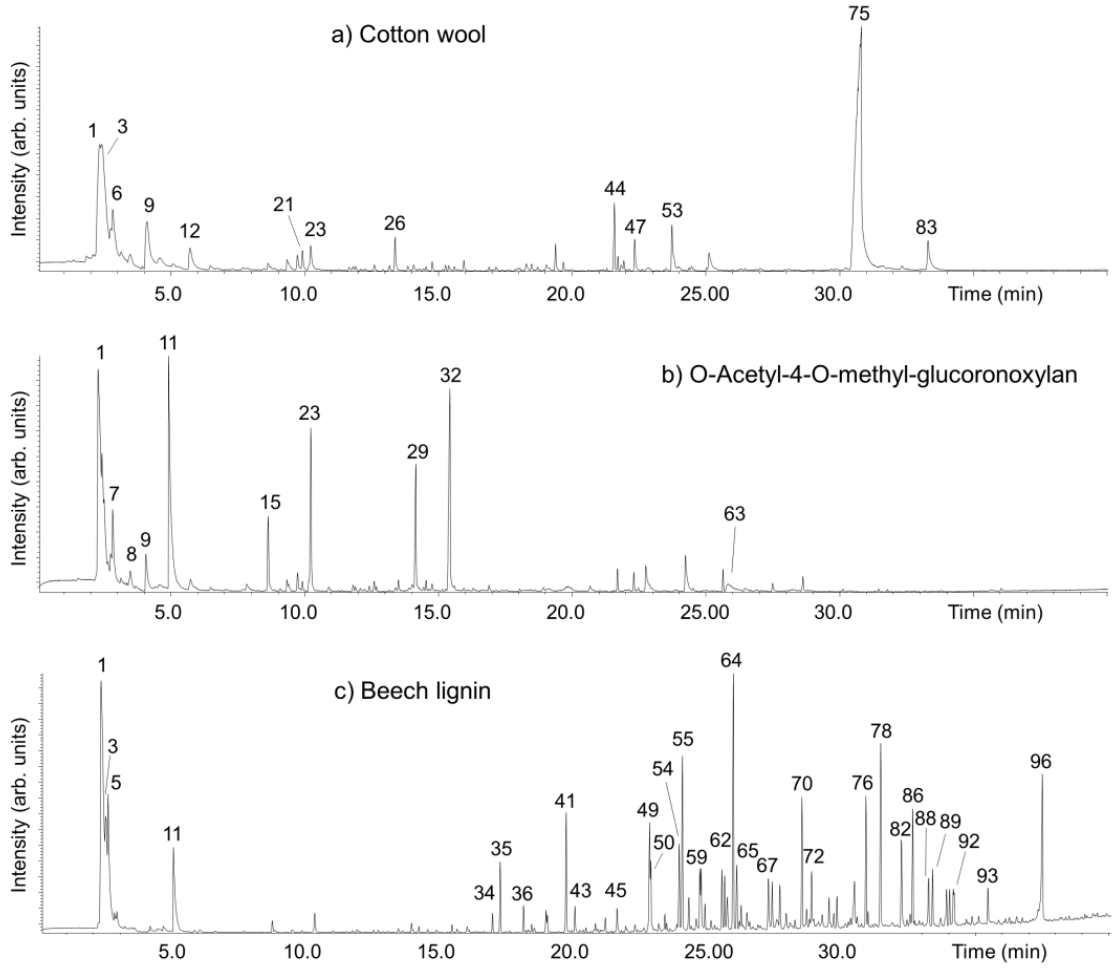

Figure 3.6. Total ion chromatograms of the pyrolysis products of Py-GC/MS experiments on (a) cotton wool; (b) O-acetyl-4-O-methyl-glucuronoxylan; and (c) beech milled wood lignin. Pyrolysis was carried out at 600°C for 20s in helium atmosphere.

The total ion chromatogram of the pyrolysis products (pyrogram) of cotton cellulose is shown in Fig. 3.6 a. The pyrolysis was carried out at 600°C for 20 s in helium atmosphere and the products were analyzed on-line with GC/MS. The identification of the pyrolysis products has been carried out using the NIST mass spectral library as well as the chromatographic retention data and mass spectra collection of Faix and coworkers [53-56]. For the identification of a few additional compounds some other papers have been used [57-62]. Table 3.3 lists the major products together with the most important mass spectrometric ions and molecular mass. As Fig. 3.6 a indicates, levoglucosan (1,6-anhydroglucopyranose) is the most important decomposition product of cellulose, and much smaller amount of 1,6-anhydroglucofuranose is formed. A few anhydrosugar products can be derived from the

Table 3.3. The main decomposition products of biomass samples during pyrolysis at 600°C, 20 s. Peak numbers refer to the peaks in Figs. 3.6 and 3.7.

Peak No.	Retention time (min)	Compound	Abundant ions (m/z)	Molar mass Da
1	2.28	Carbon dioxide	44, 28, 16	44
		+ methane	16, 15, 14	16
2	2.35	Formaldehyde	29, 30, 28, 15	30
3	2.46	Water	18, 17, 16	18
4	2.55	Acetaldehyde	29, 44, 43, 26	44
5	2.62	Acetone +	43, 58, 15, 27	58
		methanol	31, 32, 29, 15	32
6	2.84	2-Propenal	27, 56, 55, 26	56
7	2.92	Propanal-2-one	43, 29,15, 72	72
8	3.58	2,3-Butanedione	43, 86, 15	86
9	4.20	Hydroxyacetaldehyde	31, 29, 32, 60	60
10	4.65	2-Butenal	41, 70, 39, 69	70
11	5.06	Acetic acid	43, 45, 60	60
12	5.80	Hydroxypropanone	43, 31, 74	74
13	6.58	1,2-Dihydroxyethene	31, 42, 29, 60	60
14	8.48	1,2-Ethanediol	31,33, 43, 62	62
15	8.73	3-Hydroxypropanal	43, 73, 42, 74	74
16	8.81	3-Butenal-2-one	84, 27, 29, 55	84
17	8.95	(3H)-Furan-2-one	84, 55, 39, 70	84
18	9.44	(2H)-Furan-3-one	84, 54, 26, 55	84
19	9.49	3-Furanaldehyde	95, 96, 39, 67	96
20	9.83	Butanedial	58, 29, 57, 43	86
21	10.02	2-Hydroxy-butanal-3-one	43, 31, 29, 102	102
22	10.25	2-Cyclopenten-1-one	82, 54, 53, 39	82
23	10.31	2-Furanaldehyde	96, 95, 39, 29	96
24	11.70	2-Furfuryl alcohol	98, 41, 81, 39	98
25	12.68	2-Cyclopentene-1,4-dione	96, 42, 68, 54	96
26	13.44	1,2-Cyclopentanedione	98, 55, 42, 69	98
27	13.92	Dihydromethylfuranone	70, 42, 98, 39	98
28	14.07	5-Methyl-2-furanaldehyde	110, 109, 53, 81	110
29	14.15	Pyranone derivative	55, 86, 43, 56	114
30	14.77	(5H)-Furan-2-one	55, 84, 27, 54	84
31	15.34	γ-Lactone derivative	110, 85, 43, 39	110
32	15.44	4-Hydroxy-5,6-dihydro-2H-pyran-2-one	114, 58, 29, 57	114
33	16.01	1-Methyl-2-hydroxy-1-cyclopentene-3-one	112, 55, 69, 84	112
34	16.94	Phenol	94, 66, 65, 39	94
35	17.23	2-Methoxyphenol (Guaiacol)	109, 124, 81, 53	124
36	18.10	2-Methylphenol	108, 107, 77, 79	108
37	18.53	3,5-Dihydroxytoluene	124, 123, 95, 39	124

38	18.79	Dihydromethylfuranone	69, 98, 41, 39	98
39	18.95	4-Methylphenol	107, 108, 77, 79	108
40	18.99	3-Methylphenol	108, 107, 79, 77	108
41	19.70	4-Methylguaiacol	138, 123, 95, 77	138
42	19.75	Anhydrosugar	44, 57, 43, 29	
43	20.02	2,6-Dimethylphenol	107, 122, 121, 77	122
44	21.60	(1R,5S)-1-hydroxy-3,6-dioxabicyclo[3.2.1]octan-2-one	43, 41, 69, 116	144
45	21.65	4-Ethylguaiacol	137, 152, 122, 91	152
46	21.79	4-Hydroxy-3-methyl-(5H)-furanone	114, 56, 42, 84	114
47	22.38	1,4:3,6-Dianhydro-α-D-glucopyranose	69, 57, 29, 98	144
48	22.59	1,4-Anhydroarabinofuranose	57, 73, 29, 86	132
49	22.81	3-Methoxy-1,2-benzenediol	140, 125, 97, 51	140
50	22.87	4-Vinylguaiacol	150, 135, 107, 77	150
51	22.50	2,3-Dihydrobenzofuran	120, 91, 119, 65	120
52	23.40	4-Allylguaiacol (Eugenol)	164, 149, 103, 77	164
53	23.78	5-Hydroxymethyl-2-furanaldehyde	97, 126, 41, 69	126
54	23.93	1,2-Benzenediol (Cathecol)	110, 64, 81, 92	110
55	24.04	2,6-Dimethoxyphenol (syringol)	154, 139, 96, 111	154
56	24.50	Dihydro-4-hydroxy-(3H)-Furan-2-one	44, 43, 29, 74	102
57	24.58	cis-Isoeugenol	164, 149, 77, 103	164
58	24.71	3-Methyl-1,2-benzenediol	124, 78, 123, 39	124
59	24.75	3,4-Dimethoxyphenol	154, 139, 111, 65	154
60	25.16	2-Hydroxymethyl-5-hydroxy-2,3-dihydro-(4H)-pyran-4-one	144, 87, 97, 29	144
61	25.52	4-Methyl-1,2-benzenediol	124, 123, 78, 77	124
62	25.64	Trans-isoeugenol	164, 149, 77, 103	164
63	25.72	1,4-Anhydro-β-D-xylopyranose	57, 73, 29, 43	132
64	25.95	4-Methylsyringol	168, 153, 125,107	168
65	26.08	Vanillin	151, 152, 81, 109	152
66	26.30	C_3H_3-guaiacol	162, 147, 91, 119	162
67	27.27	4-Propylguaiacol	137,166, 122, 94	166
68	27.39	Anhydrosugar	45, 73, 57, 42	132
69	27.70	Acetoguaiacone	151, 166, 123, 108	166
70	28.52	4-Vinylsyringol	180, 165, 137, 122	180
71	28.70	Guaiacylacetone	137, 180, 122, 94	180
72	28.90	Allylsyringol	194, 167, 91, 119	194
73	29.24	1,6-Anhydro-α-D-galactopyranose	60, 57, 73, 29	162
74	30.31	Anhydrosugar	43, 60, 73, 57	
75	30.72	Levoglucosan	60, 57, 73, 29	162
76	30.91	trans-4-Propenylsyringol	194, 91, 179, 119	194
77	31.01	Dihydroconiferyl alcohol	137, 182, 138, 122	182
78	31.46	Syringaldehyde	182, 181, 167, 111	182

79	31.51	Cis-coniferyl alcohol	137, 180, 124, 91	180
80	31.69	Anhydrosugar	73, 57, 103, 60	
81	31.91	Anhydrosugar	43, 73, 60, 99	
82	32.24	4-Propylsyringol	167, 196, 168, 123	196
83	33.30	1,6-Anhydro-β-D-glucofuranose	73, 69, 43, 44	162
84	32.40	Anhydrosugar	45, 73, 69, 41	
85	32.57	Anhydrosugar	73, 71, 60, 87	
86	32.66	Acetosyringone	181,196, 153, 138	196
87	32.93	Trans-coniferyl alcohol	137, 180, 124, 91	180
88	33.27	Coniferyl aldehyde	178, 135, 147, 107	178
89	33.40	Syringyl acetone	167, 210, 168, 123	210
90	33.92	Propiosyringone	181, 210, 182, 153	210
91	34.04	a-Oxypropiosyringone	181, 182, 153, 224	224
92	34.18	4-(Oxoallyl)-syringol	181, 208, 55, 182	208
93	35.47	Dihydrosynapyl alcohol	168, 167, 212, 153	212
94	35.90	cis-Synapyl alcohol	210, 167, 154, 182	210
95	37.30	trans-Synapyl alcohol	210, 167, 154, 182	210
96	37.51	Synapyl aldehyde	208, 165, 137, 177	208

glucopyranose units by dehydration, e.g., 1,4:3,6-dianhydro-α-D-glucopyranose. Several furan derivatives also evolve, which may originate from the glucofuranose structure through dehydration steps. The smaller molecular mass products are mostly aldehydes and ketones, which are formed by fragmentation of the sugar units. Hydroxyacetaldehyde represents the most typical smaller product.

Fig. 3.6 b illustrates the pyrogram of O-acetyl-4-O-methylglucuronoxylan, the main hemicellulose component of hardwoods, which was isolated from beech wood [8]. Table 3.3 includes the identification of the pyrolysis products of xylan, too. The main pyrolysis product is acetic acid, which is derived from the acetyl substituents on the xylose units. From the main xylan backbone, small amounts of monomer units with pyranose structure are formed by depolymerization (1,4-anhydro-β-D-xylopyranose) due to steric reasons. However the majority of the significant products are formed by dehydration reaction. Pyranone derivatives keep the original six-membered ring structure, 4-hydroxy-5,6-dihydro-2H-pyran-2-one is a very typical pyrolysis product of xylan. Furan derivatives (e.g., 2-furanaldehyde) are also important pyrolysis products of hardwood hemicellulose. Fragmentation of the saccharide rings also occurs yielding oxo-compounds (3-hydroxypropanal, propanal-2-one etc.).

Lignin is the by-product of pulping (paper production) technology. The economic utilization of lignin is not solved, therefore numerous papers have been published on the possible thermal conversion and structural characterization of lignin [63-66]. Fig. 3.6 c presents the pyrogram of a milled wood lignin isolated from beech wood [63]. Table 3.3 shows the most important lignin products, too. During fast pyrolysis, lignin produces mainly monomeric aromatic products with preserved aromatic methoxyl and hydroxyl groups. The aliphatic side chain have up to three carbon atoms containing hydroxyl and carbonyl groups

as well as double bonds. Beech lignin has about the same amount of guaiacyl-type and syringyl-type monomeric units. During pyrolysis, beech milled wood lignin produces higher yield of syringyl-type products (e.g., 4-methylsyringol, syringol, syringaldehyde and synapyl aldehyde) than guaiacyl-type monomeric products (e.g., 4-methylguaiacol, guaiacol, 4-vinylguaiacol, vanillin, coniferyl aldehyde). Synapyl and coniferyl alcohols and aldehydes keep the original 3 aliphatic carbon atoms on the aromatic ring, thus they are markers of the original lignin structure.

3.4.3. Pyrolysis of Whole Biomass Samples

Hundreds of papers have been published on the analytical pyrolysis of various biomass samples for structural studies or for possible utilization purposes, only a few of them are cited here [42,67-72]. Typical pyrograms of a softwood, a hardwood and a herbaceous plant are illustrated in Fig. 3.7.

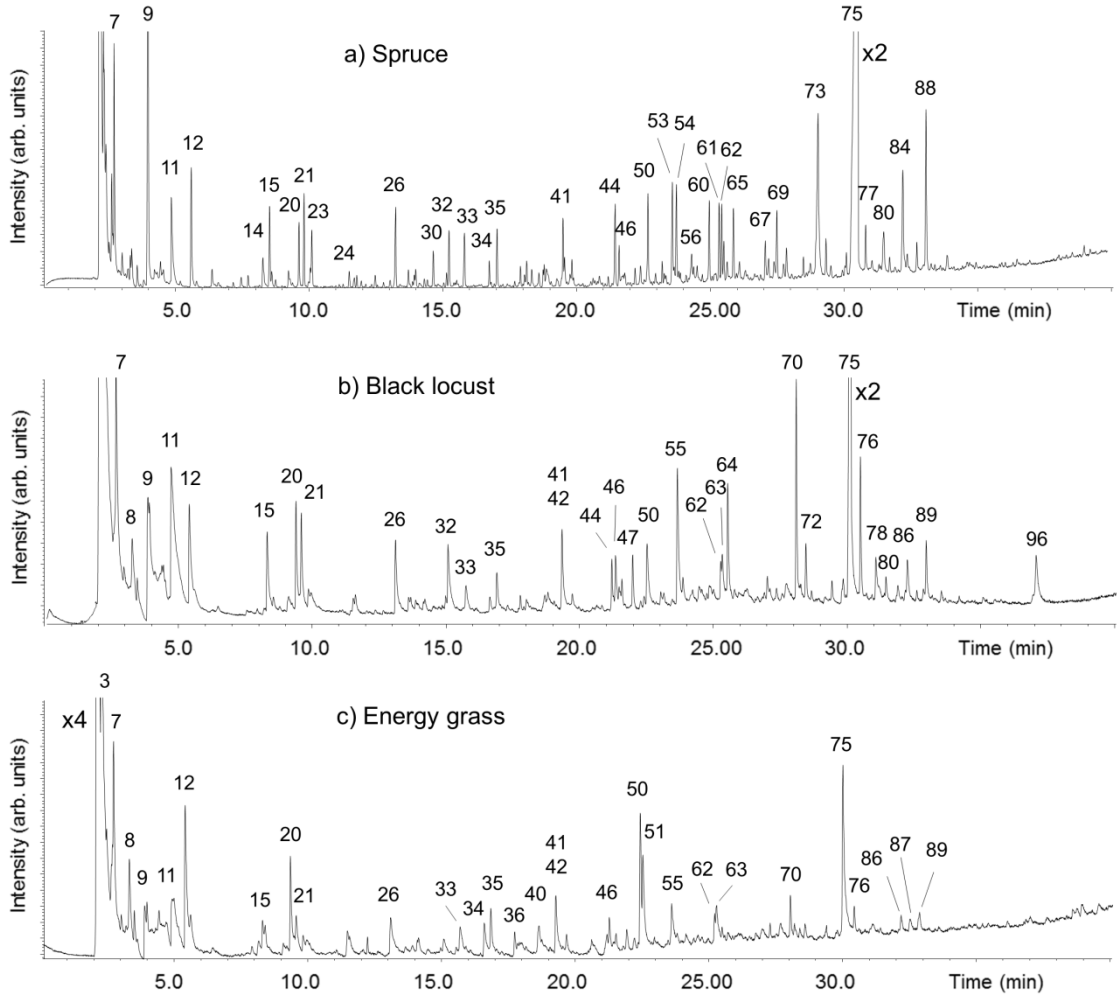

Figure 3.7. Total ion chromatograms of the pyrolysis products of Py-GC/MS experiments on (a) spuce wood; (b) black locust wood; and (c) energy grass. Pyrolysis was carried out at 600°C for 20s in helium atmosphere.

During pyrolysis of biomass samples, more than a hundred chemical compounds are formed, which is one of the main problems of the utilization of biooils. The identification of the most important products is listed in Table 3.3. In addition to a few gaseous products, levoglucosan represents the main decomposition product from the cellulose component of each biomass samples. Its intensity is much higher from the wood samples than from the herbaceous plant due to the lower inorganic content of wood, as will be discussed later. However, levoglucosan yield is lower from biomass samples in comparison with the pure cellulose taking into account the cellulose content of biomass. As shown in Fig. 3.7 a, spruce produces high yield of hydroxyacetaldehyde. Several other oxo-compounds and furan derivatives are released from each samples indicating the fragmentation of the sugar units. Quite a few anhydrosugars were detected, some of them were not identified. 1,4-anhydro-β-D-xylopyranose is a depolymerization product of xylan, which is the main hemicellulose in hardwoods, but it is present in the energy grass, too. Spruce evolves relatively high yield of 1,6-anhydro-α-D-galactopyranose, which is a characteristic depolimerization product of the softwood hemicelluloses. Dehydration of the sugar moieties of cellulose and hemicellulose leads to the formation of pyranone derivatives.

Phenolic compounds dominate in the pyrogram after 16 min. retention time, indicating the presence of the lignin components of the biomass. Spruce contains only coniferyl monomeric units, hence it produces various methoxyphenolic (guaiacol) compounds. The highest molecular mass product of lignin origin is coniferylaldehyde. Significant amount of cathecol and alkylcathecols are also formed indicating the demethylation of the methoxyl groups at 600°C pyrolysis temperature. From black locust, higher yields of syringol (dimethoxyphenol) derivatives are released than guaiacol compounds similarly to the milled wood lignin of beech. Energy grass produces the highest yields of guaiacol derivatives followed by syringol compounds. Some phenol and methylphenols are also evolved from the so-called H-lignin moieties.

3.5. REACTION MECHANISM OF THE THERMAL DECOMPOSITION

3.5.1. Cellulose Decomposition

Most of the proposed mechanisms for cellulose and biomass pyrolysis are based on hypotheses instead of unambiguous proofs. Nevertheless, consideration of the various alternatives provides an insight into the possible carbohydrate reactions. It is generally agreed [2, 18] that two competing reactions occur during the pyrolysis of cellulose: the first is a fragmentation reaction to generate char and light volatile products (including gases, water, aldehydes, ketones etc.) and the second is a depolymerization to yield primarily levoglucosan, as well as other anhydromonosaccharides. The first reaction pathway is more important at low temperatures and slow heating rates, while the second pathway dominates at higher temperatures and at higher heating rates. This model is a simplification of extremely complex chemical and physical phenomena, which means that a partial reaction in the scheme may correspond in reality to a group of reactions. Shafizadeh and co-workers [2, 6] as well as Broido and Nelson [73] have proposed a model for cellulose pyrolysis, in which the formation of an "active cellulose" is assumed to be the primary step before the above mentioned two steps. Applying prolonged thermal pretreatments of Avicel cellulose followed

by thermogravimetric analysis, Várhegyi *et al*. [74] concluded that the experimental results are better represented with kinetic models which exclude the initiation reaction.

The formation of the major volatile products can be explained by simplified reaction mechanisms. Pakhomov [75] suggested a free-radical mechanism for the release of levoglucosan during the thermal decomposition of cellulose in vacuum. It is not agreed in the literature, whether the initial scission occurs within the chain [75] or at the chain end [47]. Scheme 3-1 shows a free radical mechanism with the chain scission of the macromolecule. The free-radical peeling reactions involve initial cleavage of the oxygen bond at C-4 bond (β-(1-4) glycosidic bond), hydrogen transfer from the C-6 hydroxyl group to C-4, and the formation of an oxygen bridge between C-6 and C-1. This mechanism is supported by the fact that considerable amount of levoglucosan is evolved from starch, too, where similar radicals are formed after the cleavage of the α-(1-4) glycosidic bonds [76]. Kilzer and Broido [18] proposed that 1,4-anhydro compound is formed as an intermediate and it is rearranged to 1,6-anhydro-glucopyranose or 1,6-anhydro-β-D-glucofuranose according to whether the C-6 hydroxyl group attacks the 1,4 or 1,5 ring of the intermediate compound.

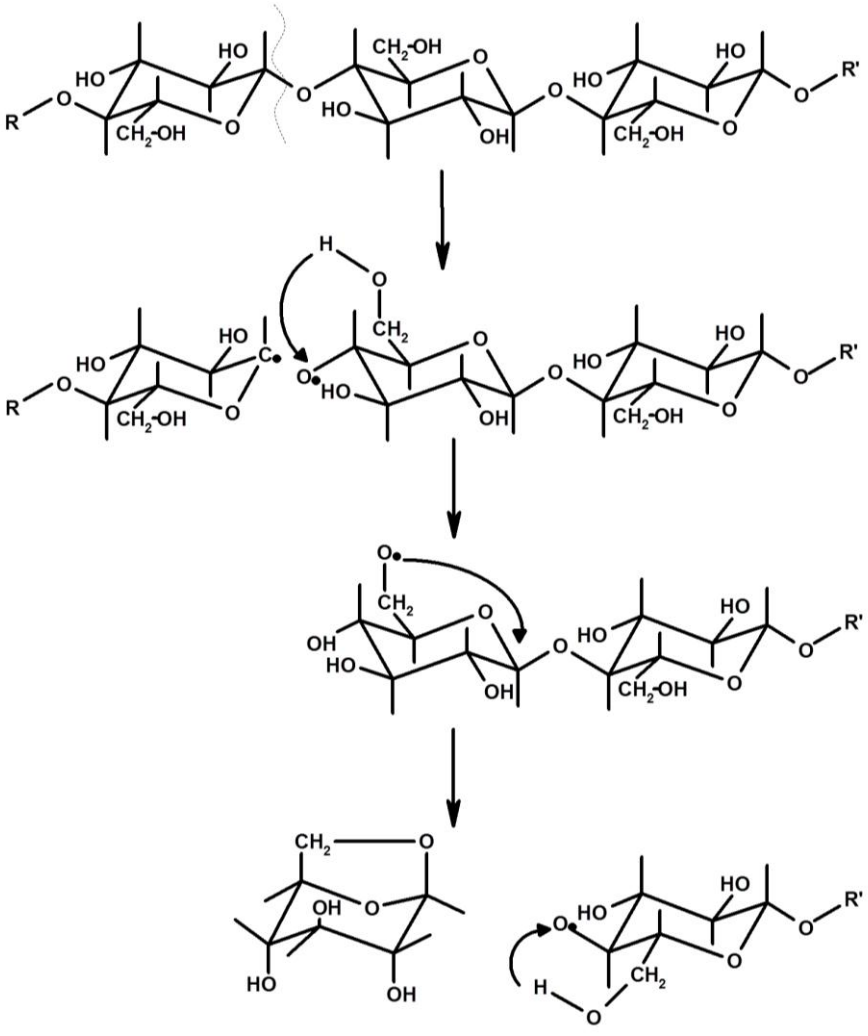

Scheme 3.1. Depolymerization mechanism of cellulose during pyrolysis.

Mamleev *et al*. [47] suggested a two-level kinetic model for cellulose pyrolysis. According to the hypothesis, tar and volatile acids are released during the first transglycosylation step due to the decomposition of the non-reducing chain ends. The volatile acids catalyze various heterolytic reactions including the formation of light gases as a result of fragmentation and depolymerization by the acid-catalyzed β-elimination. An argument against this hypothesis is that very high yield of levoglucosan is released during vacuum pyrolysis, where there is no acid catalyst.

Recently three mechanisms for levoglucosan formation during cellulose pyrolysis have been studied by Zhang *et al*. [77], which are the free-radical mechanism, glucose intermediate mechanism, and levoglucosan chain-end mechanism. Based on activation energy calculations, it was concluded that levoglucosan chain-end mechanism which happens via two transglycosylation steps is the most reasonable pathway from the three mechanisms for levoglucosan formation.

Another major product of cellulose pyrolysis is hydroxyacetaldehyde (glycolaldehyde), which more likely forms directly from the cellulose chain [78] than from levoglucosan [2, 79]. Richards [78] suggested a retro-Diels-Alder reaction mechanism for the elimination of hydroxyacetaldehyde after dehydration of a glucose segment in cellulose. According to this mechanisms, glycolaldehyde is predominantly derived from C5 and C6 segments of a monomer unit. as shown in Scheme 3-2.

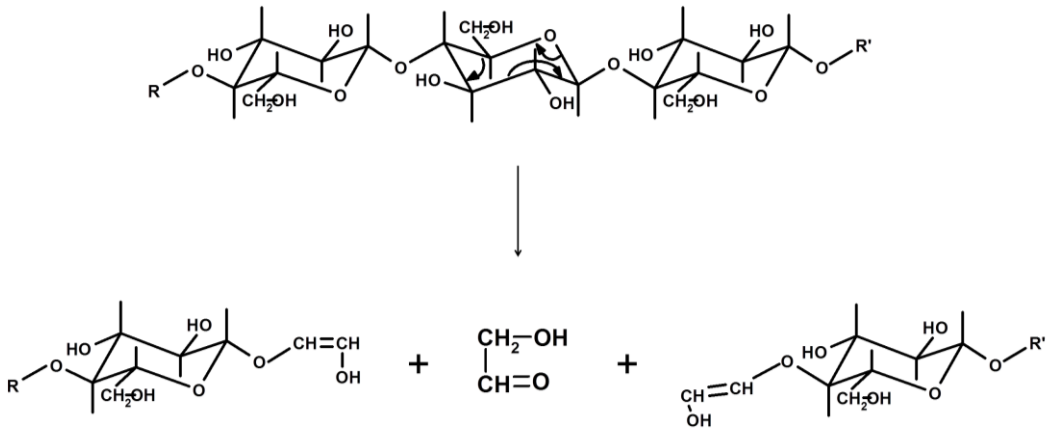

Scheme 3.2. Formation of hydroyacetaldehyde by reverse aldolization during cellulose pyrolysis.

Arisz and Boon [80] studied the pyrolysis of cellulose derivatives and observed that the E_i-elimination reaction plays key role in those molecules where the 6-O-positions in the cellulose backbone are substituted. This reaction is suggested to occur during cellulose decomposition to a smaller degree (Scheme 3-3). It is confirmed by the low yield of pyranone derivatives in the pyrolyzate. On the other hand, high water yield suggest the dehydration of the sugar units to a high degree. Other dehydrated products are the furan derivatives, which adds to the water formation, too.

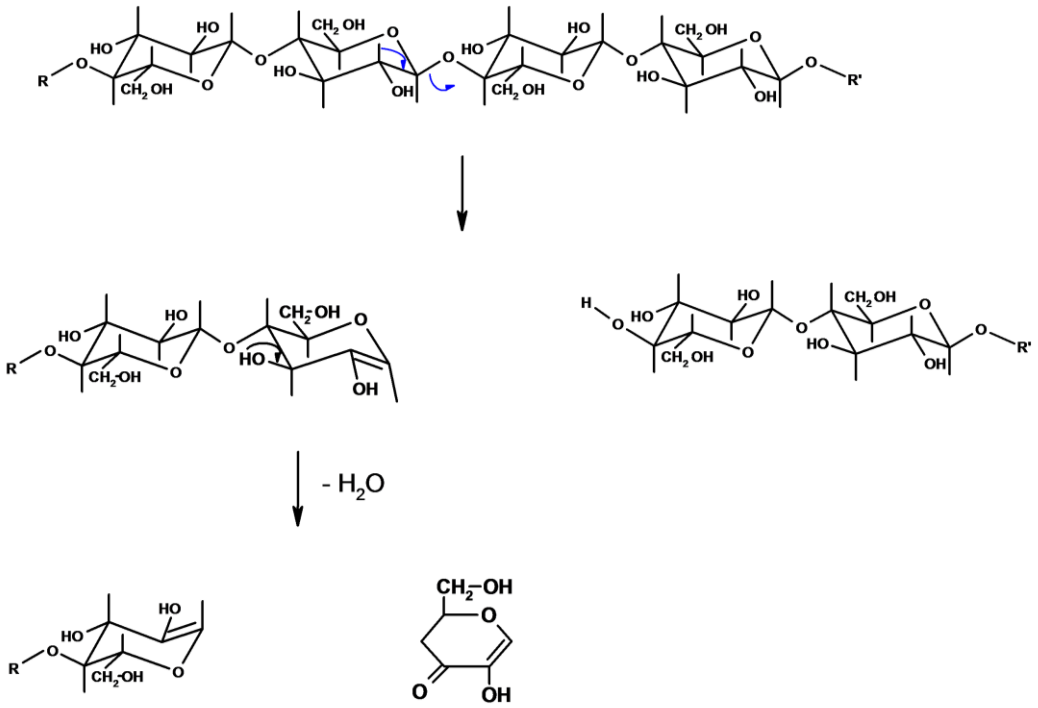

Scheme 3.3. Formation of pyranone rings during cellulose pyrolysis.

3.5.2. Hemicellulose Decomposition

Less literature data are available for the hemicellulose decomposition due to the difficult isolation procedures of hemicelluloses. It is assumed that hemicellulose decomposes according to similar dissociation and fragmentation mechanisms as cellulose during pyrolysis. The monomeric building blocks of hemicellulose form anhydrosugars, which retain the configuration of the original saccharide units [59, 60,81]. The most common hemicellulose in softwoods is mannan, which contains mainly mannopyranose segments, but it has galactopyranose and glucopyranose units, too. During pyrolysis, the anhydro derivatives of the sugar units are formed. Xylan represents the major hemicellulose in hardwoods, which produces mostly 5,6-dihydro-4-hydroxy-2H-pyran-2-one in addition to 1,4-anhydroxylopyranose (Scheme 3-4). Several common furanoic carbohydrate pyrolysis products are also obtained from hemicelluloses; Scheme 3-4 illustrates the possible formation route of 2-furanaldehyde. Recently Shen *et al*. [15] studied the pyrolysis of O-acetyl-4-O-methylglucorono-xylan isolated from beech wood. The formation of furfural and 1,4-anhydro-D-xylopyranose was attributed mainly to the xylan units. Due to the smaller stability of 1,4-anhydro-D-xylopyranose it decomposes by the rearrangement leading to the formation of furan derivatives. Acetic acid and carbon dioxide were assumed to be released from the primary decomposition of O-acetylxylan segments. The xylan unit is also the main precursor for the formation of the two-carbon, three-carbon fragments and gases (carbon monoxide, hydrogen and methane). The evolution of methanol is mainly ascribed to the primary reactions of 4-O-methylglucoronic acid unit, which could be further decomposed to almost all of the products generated from the other two units.

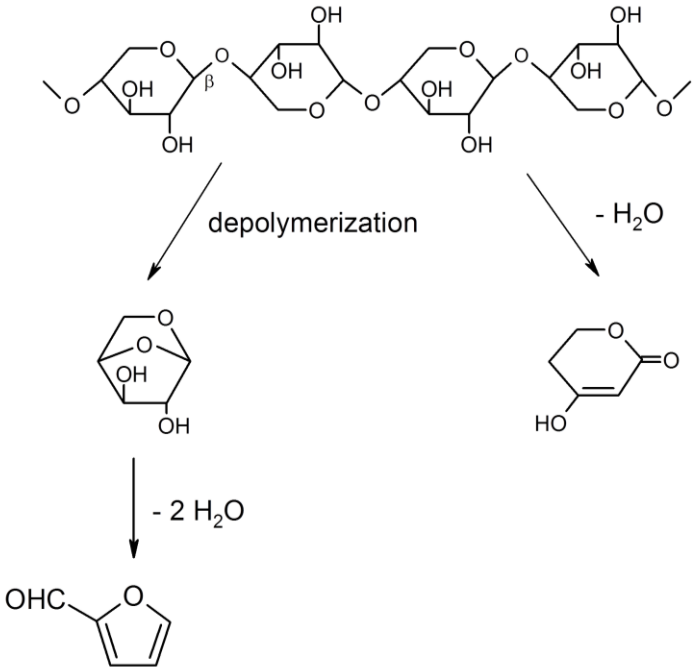

Scheme 3.4. Dehydration reactions of xylan units during pyrolysis.

3.5.3. Lignin Decomposition

Due to the complexity of the lignin structure, it is difficult to understand its pyrolysis mechanisms. Therefore, several studies have been carried out to discover the primary reactions on lignin model compounds [82-87]. A comparison of the products from the pyrolysis of lignin, biomass, and the surface-immobilized model compounds provided evidence that the thermal degradation of lignin occurs principally by a free-radical reaction pathway [85]. It was clarified that the ether bond is prone to be cleaved easily [87]. Britt *et al.* [84] concluded that methoxyl substituents enhance the homolysis of the β-O-4 linkage. The methoxyl-substituted phenoxy radicals undergo a complex series of reactions, which are dominated by intramolecular hydrogen abstraction, rearrangement, and β-scission reactions.

During the slow thermal decomposition of lignin - as it is the case in the TGA experiments - the cleavage of functional groups plays an important role leading to the evolution of low molecular mass products (20-25 % m/m) and the formation of char (25-40 % m/m). Correlations have been found between the abundance of volatile products and the type and amount of functional groups [88] using lignin samples prepared by different isolation techniques. The terminal CH_2OH groups decompose by the release of both water and formaldehyde as demonstrated by the relationship between the aliphatic OH-group content and the formaldehyde as well as the water evolution. The dependence of the methane yield on the methoxyl group content provided evidence that the scission of methoxyl groups results in the formation of methane as well as methanol.

Beside the cleavage of the functional groups, the formation of monomeric or dimeric lignin products represent about 40-50% of the total pyrolysis yield. Similarly to the model compounds, generally the β-4-O bonds are cleaved, but the aliphatic side groups are also

partially or fully removed. Thus, numerous aromatic products, mostly phenolic compounds are evolved as indicated on the pyrogram of milled wood beech lignin (Fig. 3.6 c) and Table 3.3. Recently Mu *et al*. reviewed the pyrolysis products and the possible mechanisms of lignin decomposition [89] focusing on the upgrading possibilities of the pyrolysis oil.

3.5.4. Mechanisms of Biomass Pyrolysis

Levoglucosan can be obtained from cellulose in yields from 20 to 70% by weight [3, 46]. However, from lignocellulosic biomass materials the yields of levoglucosan are less than 5%, although the cellulose content is about 40%. Nevertheless, it is generally assumed that the thermal decomposition of biomass samples occurs by parallel reactions of the degrading components. The presence of inorganic ions (mostly potassium) reduces the levoglucosan yield to a certain extent. However, the low yield of levoglucosan from inorganic-free biomass samples indicates that the presence of other components enhances the secondary reactions of the primary decomposition products.

3.6. EFFECT OF INORGANIC MATERIALS ON THE DECOMPOSITION MECHANISM

The biomass materials, in addition to the main macromolecular components, contain different amount of extractable materials (e.g., resins, fats, terpenes and flavonoids) as well as inorganic components. The extractive materials partly evaporate, partly decompose during the thermal decomposition, however they do not exert significant influence on the thermal decomposition mechanisms of the macromolecular components [90]. The inorganic content is generally determined as ash, which varies in a wide range depending on the type of biomass. Wood samples contain rather low inorganic content (0.5-1-5%), but the bark of wood has 2-5% inorganic compounds [1]. The herbaceous biomass samples contain generally higher amount of inorganic compounds (about 4-16%). Calcium and potassium are the predominant cations, which are mostly found in carbonate, silicate, oxalate salts. Other elements are also found in biomass, such as magnesium, sodium, phosphorus, iron, aluminum and several trace elements.

The early studies focused on the flame retardant effect of inorganic compounds on biomass materials during combustion [6, 10]. The flame retardant effect results primarily from the tendency of certain inorganic materials to lower the decomposition temperature of the substrate, which favors carbonization rather than depolymerization of the macromolecules resulting in higher char yield. Hence, less volatile materials are available for the gas phase combustion. During pyrolysis, the inherent inorganic components of biomass materials have significant influence on the decomposition mechanisms. Potassium is a key plant nutrient, whose concentration is the highest in the herbaceous plants. Of all the metals present in biomass, potassium has the greatest effect on the thermal decomposition mechanisms. Among the biomass components, cellulose is the most susceptible for the presence of inorganic ions during the thermal decomposition. Therefore, numerous studies have been carried out on the effect of alkali ions on the pyrolysis of cellulose [10, 48], lignocellulosic materials [91, 92] and model compounds [93]. Demineralized [94], cation-exchanged [11] and impregnated [91, 92, 95, 96] cellulose, wood and herbaceous biomass samples have been

studied. It was concluded that the presence of potassium and sodium promote gas and char formation at the expense of the tar yield during cellulose pyrolysis. Especially the levoglucosan yield is reduced in the presence of alkali metal ions indicating that the depolymerization reactions are hindered, while the fragmentation reactions of the sugar moieties to low molecular weight components (e.g., water, methane, carbon oxides, hydroxacetaldehyde) are enhanced [48, 93].

It is well known that the catalytic effect depends on the amount of alkali ions since the herbaceous samples of high inorganic contents produce much higher char yield than the wood samples of low ash content [61, 97-100]. The effect of alkali ion concentration has been studied in detail on the thermal decomposition of hemp by Sebestyén *et al*. [101] Fig. 3.8. presents the effect of potassium and sodium content on a few thermogravimetric and mass spectrometric parameters of untreated, hot water washed, and alkali-treated hemp samples.

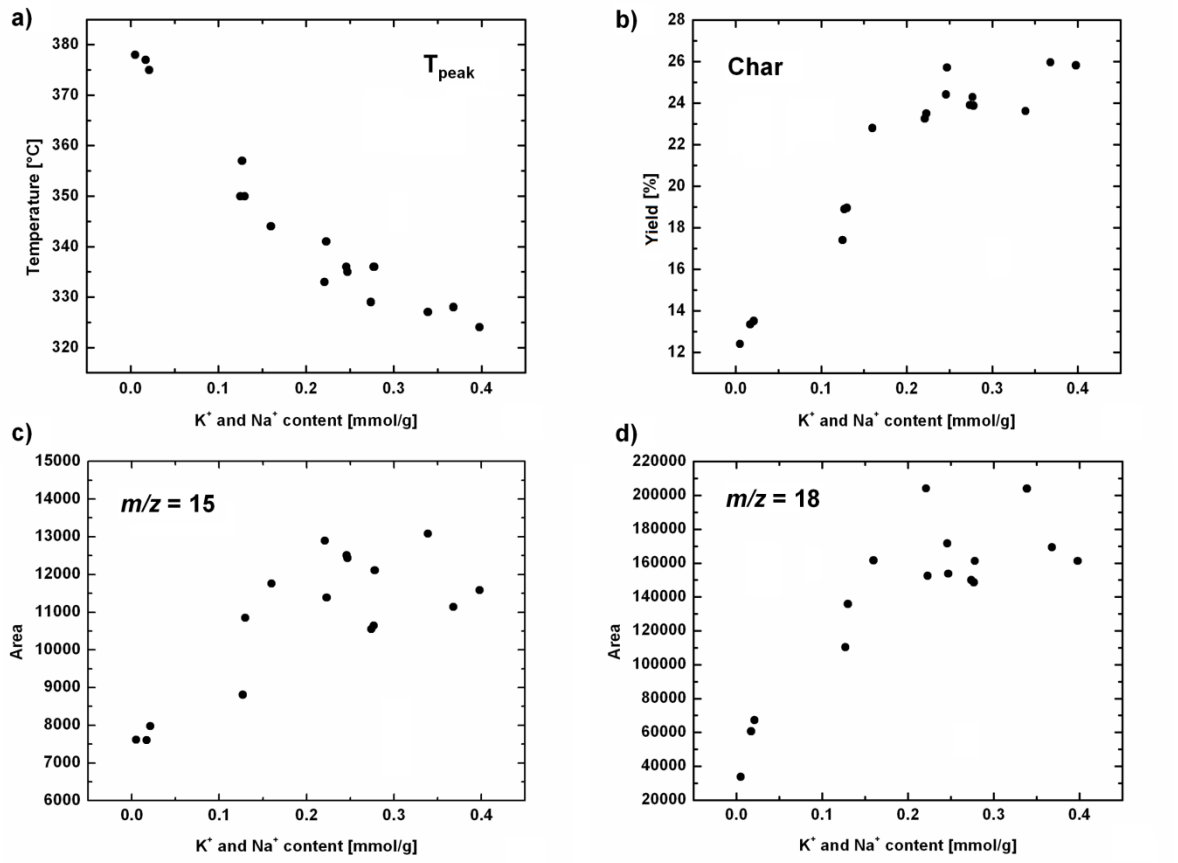

Figure 3.8. Relationships between the TG/MS parameters of native, hot-water washed and alkaline-treated hemp and the alkali ion contents (K^+ + Na^+) of the samples. (a) Temperature of the DTG peak maximum; (b) char yield; (c) integrated intensity of methane peak (*m/z* 15); (d) integrated intensity of water peak (*m/z* 18). Figure is taken from ref. 101 with the permission of Springer.

The alkali ion content was determined using inductively coupled plasma-optical emission spectroscopy method. The changes in the parameters as a function of the alkali ion concentration is not linear; the steepest alteration in the TG/MS parameters can be observed in the 0–0.2 mmol/g concentration range of the alkali ions followed by a gradual decrease in

the effect in the higher concentration range. The DTG peak of the cellulose constituent of hemp shifts to lower temperature in the case of alkali-containing samples. The temperature of the maximal decomposition rate (T_{peak}) reduces from 380 to 320°C (Fig. 3.8 a), and the char yield (Fig. 3.8 b) is doubled as the alkali ion concentration increases from 0 to 0.4 mmol/g. On the other hand, the yield of low molecular mass products increases significantly: methane evolution is almost doubled (Fig. 3.8 c) and the water yield shows about a sixfold increase (Fig. 3.8 d). Methane formation can be attributed to the charring process, while water is forming at lower temperatures by the scission of the hydroxyl functional groups.

The influence of potassium on the cellulose decomposition mechanism is quite well understood, but the effect on the pyrolysis of other cell-wall components in biomass are much less established. Nowakowski *et al*. [93] studied the pyrolysis of oat spelt xylan, a typical hemicellulose, in the presence of potassium and found little effect on the thermogravimetric curves and the pyrolysis product distribution. It has been proposed that the negligible effect is due to the alkali metal content of the raw xylan, which is introduced during the isolation.

A systematic study of the effect of cations on the thermal decomposition of lignins was performed by Jakab *et. al*. [16, 102, 103]. It was shown that the addition of sodium enhances dehydration, demethoxylation, decarboxylation, and char formation, whereas it decreases the yield of higher molecular mass volatiles and carbon monoxide formation. The presence of $ZnCl_2$ has significant effect on the thermal decomposition of milled wood lignins as detected by TG/MS [16]. The evolution of water and formaldehyde shifts to 60-80°C lower temperature indicating a substantial alteration of the decomposition mechanisms in the presence of the Lewis acid. The addition of $ZnCl_2$ to pine lignin isolated from a rotting log, reduced the relative abundance of coniferyl alcohol released, while the relative intensity of guaiacol and 4-methylguaiacol increased using pyrolysis-mass spectrometry with molecular-beam sampling [66]. This finding supports the conclusion of Jakab *et al*. [16] that the terminal -CH_2OH groups are prone to be cleaved in the presence of sodium or zinc ions. The effect of potassium on the lignin pyrolysis was confirmed by Nowakowski *et al*. [93], which was indicated by the increased char yield and a lower temperature decomposition in the presence of potassium.

Various inorganic compounds can be added to biomass samples in order to enhance the yield of a certain product and reduce the number of the pyrolysis products [104, 105]. Catalytic conversion is discussed in a separate chapter. Here, only a few special reactions are mentioned. When cellulose pyrolysis is catalyzed by nanopowder titanium dioxide, aluminum oxide and aluminum titanate [57, 58, 106], a high yield of a chiral hydroxylactone ((1R,5S)-1-hydroxy-3,6-dioxabicyclo[3.2.1]octan-2-one) is formed, which is suggested for the use in chiral syntheses.

Mild acidic additives during pyrolysis can also be used for modifying the pyrolysis product distribution of carbohydrates. Shafizadeh and Chin [13] established that cellulose pyrolysis yielded mostly levoglucosan and only small amount of dehydration products (e.g., 1,4:3,6-dianhydro-α-D-glucopyranose). When the pyrolysis of cellulose was carried out in the presence of acidic catalysts, a substantial amount of a dehydrated product, levoglucosenone were evolved. Strong acids lead to hydrolysis of carbohydrate therefore mild acids, can be used during catalytic pyrolysis. The highest yield of levoglucosenone was achieved with the use of phosphoric acid [107, 108]. Levoglucosenone is an optically active

compound suited for the synthesis of biologically active products, and it is a promising monomer for the chemical and pharmaceutical industry.

Alkaline pretreatments may be used during thermal decomposition for modifying the reaction mechanisms. Alkaline activation during charcoal preparation from biomass enhances the production of nanoporous carbon materials [109].

3.7. EFFECT OF TORREFACTION ON THE COMPOSITION AND DECOMPOSITION MECHANISMS

Torrefaction is a mild thermal pretreatment between 200 and 300°C for the conversion of biomass in an inert atmosphere. Although the low-temperature thermal pretreatments have been studied earlier [110-113], the amount of publications on torrefaction has been relatively small. However, the number of publications has increased rapidly in the last few years due to the recognition that the thermal pretreatment has economic importance in the development of efficient biomass conversion technologies.

The utilization of biomass in energetic processes has several disadvantages due to the high oxygen content, low calorific value, hydrophilic nature and the high moisture content of biomass, which makes the process design and control more complicated. Furthermore, the agricultural production of biomass involves high logistics and transportation costs due to the low energy density of biomass. These disadvantages can be reduced by the torrefaction pretreatment.

The purpose of the pretreatment from a chemical point of view is the removal of water and the acidic groups of hemicelluloses or the whole hemicellulose fraction with minor degradation of cellulose and lignin in the biomass. During the process, water and a part of the volatiles are released, causing a decrease in mass, but an increase in the energy density. A typical mass and energy balance for the torrefaction of woody biomass is that 70% of the mass is retained as a solid product, containing 90% of the initial energy content. The other 30% of the mass is converted into torrefaction volatiles, which contains only 10% of the energy of the biomass [114]. The removal of moisture reduces the microbial activity, e.g., the likelihood of rotting is diminished due to the more hydrophobic character of torrified biomass, so the storage and transportation become easier. The grindability of torrefied biomass is significantly improved when torrefaction is performed at higher temperature [115].

The pyrolysis oil produced from untreated biomass contains many oxygenated compounds including various acids, which causes the instability of the biooil. The pyrolysis oil produced from biomass pretreated by torrefaction is more stable due to the removal of acidic groups during the pretreatment [116]. Several authors studied the composition of the biooil formed from torrified biomass [116-118]. Py-GC/MS analysis exhibited [117] that the yields of acetic acid and-other lightweight compounds were lower in pyrolysis of torrefied wood, while the yields of levoglucosan in torrefied biomass pyrolysis were obviously higher due to the increased cellulose content. The char yield is obviously higher from torrified biomass owing to the increased lignin content. At lower torrefaction severity, the moisture and the hemicellulose component (e.g., acetic acid, furanaldehyde) are devolatilized, and the cellulose and lignin start to decompose with increasing temperature and time. The presence of

steam reduces the torrefaction temperature and/or time required for a given result, that is called wet torrefaction or hydrothermal treatment [119-121]. Apparently, water promotes the hydrolysis of acidic groups and hemicellulose molecules, thus enhancing the torrefaction rate.

Various substrates have different reactivity in torrefaction similarly to the different thermal stability of biomass samples. Deciduous xylan-containing wood (beech and willow) and straw are more reactive in the torrefaction process than coniferous wood [111].

Acknowledgments

This work was supported by the Hungarian National Research Fund (OTKA K81959 and K83770) as well as by the National Development Agency (Grant No. KTIA_AIK-12-1-2012-0014). My coworkers Dr. Zs. Czégény, Z. Sebestyén, Dr. J. Bozi, Dr. E. Mészáros, Á. Bora, G. Bakos and Dr. Z. May are gratefully thanked for carrying out the TG/MS, Py-GC/MS, and ICP-OES experiments. Prof. M. J. Antal, Jr., Prof. O. Faix, and Dr. A. Oudia are acknowledged for kindly providing the samples.

References

1. Sjöström, E. (1981). "Wood Chemistry. Fundamentals and Applications." Academic Press, Inc., New York, London.
2. Shafizadeh, F. (1982). Introduction to pyrolysis of biomass. Review, *J. Anal. Appl. Pyrolysis*, **3**, 283-305.
3. Shafizadeh, F., Bradbury, G.W., (1979). Thermal degradation of cellulose in air and nitrogen at low temperatures, J. Appl. Polym. Sci., **23**, 1431-1442.
4. Statheropoulos, M., Liodakis, S., Tzamtzis, N., Pappa, A., Kyriakou, S. (1997). Thermal degradation of Pinus halepensis pine-needles using various analytical methods. J. Anal. Appl. Pyrolysis **43**, 115-123.
5. Faix, O., Jakab, E., Till, F., and Székely T. (1988). Study on low mass thermal-degradation products of milled wood lignins by thermogravimetry-mass-spectrometry. Wood Sci. Technol. **22**, 323-334.
6. Shafizadeh, F. (1968). Pyrolysis and combustion of cellulosic materials, Adv. Carbohydr. Chem. Biochem. **23**, 419–474.
7. Shafizadeh, F., Furneaux, R.H., Cochran, T.G., Scholl, J.P., Sakai, Y. (1979). Production of levoglucosan and glucose from pyrolysis of cellulosic materials, J. Appl. Polym. Sci. **23.** 3525-3539.
8. Puls, J., (1997). Chemistry and biochemistry of hemicelluloses: Relationship between hemicellulose structure and enzymes required for hydrolysis, Macromolecular Symposia, **120**, 183-196.
9. Björkman A. (1957). Studies on finely divided wood. Part 3. Extraction of lignin–carbohydrate complexes with neutral solvents. Sven Papperstidn **60**, 243–251.
10. Sekiguchi, Y., and Shafizadeh, F. (1984). The effect of inorganic additives on the formation, composition and combustion of cellulosic char, J. Appl. Polym. Sci. **29**, 1267–1286.

11. DeGroot, W.F., Shafizadeh, F. (1984). The influence of exchangable cations on the carbonization of biomass, J. Anal. Appl. Pyrolysis, **6**, 217-232.
12. Choi, J.W., Choi, D-H., and Faix, O. (2007). Characterization of lignin–carbohydrate linkages in the residual lignins isolated from chemical pulps of spruce (Picea abies) and beech wood (Fagus sylvatica), J. Wood Sci. **53**, 309–313.
13. Shafizadeh, F., and Chin, P.P.S. (1976). Pyrolytic production and decomposition of 1,6-anhydro-3,4-dideoxy-b-D-glycero-hex-3-enopyranos-2-ulose. Carbohydr. Res. **46**, 149-154.
14. Jakab, E., Faix, O., Till, F., and Székely, T, (1991), Thermogravimetry/mass spectrometry of various lignosulfonates as well as of a Kraft and Acetosolv lignin, Holzforschung, **45**, 355-360.
15. Shen D.K., Gu S., Bridgwater A.V. (2010). Study on the pyrolytic behaviour of xylan-based hemicellulose using TG-FTIR and Py-GC-FTIR. J. Anal. Appl. Pyrolysis **87**, 199–206.
16. Jakab, E., Faix O., and Till, F. (1997). Thermal decomposition of milled wood lignins studied by thermogravimetry/mass spectrometry, J. Anal. Appl. Pyrolysis, **40-41**, 171-186.
17. Madorsky, S. L., Hart, V. E., Straus, S. (1958). Thermal degradation of cellulosic materials, J. Res. Nat. Bur. Standards, **60(4)**, 343.
18. Kilzer, F.J. and Broido, A. (1965). Speculations on the nature of cellulose pyrolysis, Pyrodynamics, **2**, 151-163.
19. Várhegyi, G., Antal, M.J. Jr., Jakab, E., Szabó, P., (1997). Kinetic modeling of biomass pyrolysis, J. Anal. Appl. Pyrolysis, **42**, 73-87.
20. Antal, MJ; Várhegyi, G; Jakab, E. (1998) Cellulose pyrolysis kinetics: Revisited**.** Ind. Eng. Chem. Res. **37,** 1267-1275.
21. Conesa, J.A., Caballero, J.A., Marcilla, A. Font, R. (1995). Analysis of different kinetic-models in the dynamic pyrolysis of cellulose, Thermochim. Acta **254**. 175.
22. Gronli, M; Antal, MJ; Varhegyi, G. (1999). A round-robin study of cellulose pyrolysis kinetics by thermogravimetry. Industrial & Engineering Chemistry Research, **38(6)**, 2238-2244.
23. Milosavljevic, I; Suuberg, EM, (1995). Cellulose thermal-decomposition kinetics - global mass-loss kinetics, Industrial & Engineering Chemistry Research **34(4)**, 1081-1091.
24. Bilbao, R., Millera, R. A., Arauzo, J. (1989). Kinetics of weight loss by thermal decomposition of xylan and lignin. Thermochim. Acta **143**, 137−148.
25. Várhegyi, G., Antal, M. J., Székely, T., Szabó, P. (1989). Kinetics of the thermal decomposition of cellulose, hemicellulose and sugar cane bagasse. Energy Fuels **3**, 329−335.
26. Di Blasi, C., Lanzetta, M. (1997). Intrinsic kinetics of isothermal xylan degradation in inert atmosphere. J. Anal. Appl. Pyrolysis **40−41**, 287−303.
27. Branca, C., Di Blasi, C., Mango, C., and Hrablay, I. (2013). Products and Kinetics of Glucomannan Pyrolysis, Ind. Eng. Chem. Res., 52, 5030−5039.

28. Várhegyi, G., Grønli, M.G., and Di Blasi C., (2004). Effects of sample origin, extraction, and hot-water washing on the devolatilization kinetics of chestnut wood, Ind. Eng. Chem. Res.**, 43**, 2356-2367.
29. Conesa, Juan A.; Domene, A. (2011). Biomasses pyrolysis and combustion kinetics through n-th order parallel reactions, Thermochimica Acta **523(1-2)**, 176-181.
30. Ranzi, E., Cuoci, A., Faravelli, T., Frassoldati, A., Migliavacca, G., Pierucci, S., Sommariva, S., (2008). Chemical Kinetics of Biomass Pyrolysis, Energ. Fuels, **22(6)**, 4292-4300.
31. Manya, JJ; Velo, E; Puigjaner, L, (2003). Kinetics of biomass pyrolysis: A reformulated three-parallel-reactions model, Ind. Eng. Chem. Res. **42(3)**, 434-441.
32. Miller, RS; Bellan, J., (1997). A generalized biomass pyrolysis model based on superimposed cellulose, hemicellulose and lignin kinetics, Conb. Sci. Techn., **126(1-6)**, 97-137.
33. Barneto, A.G., Carmona, J.A., Alfonso, J.E.M., Conesa, J.A., (2009). Use of Thermogravimetry/Mass Spectrometry Analysis to Explain the Origin of Volatiles Produced during Biomass Pyrolysis, Ind. Eng. Chem. Res., **48(15)**, 7430-7436.
34. Rahul S. C., Kataki, R., and Bhaskar, T. (2013). Thermogravimetric and decomposition kinetic studies of Mesua ferrea L. deoiled cake. Biores. Technol. **139**, 66-72.
35. Caballero, J.A., Conesa, J.A., Font, R., Marcilla, A. (1997). Pyrolysis kinetics of almond shells and olive stones considering their organic fractions, J. Anal. Appl. Pyrolysis **42**, 159-175.
36. Reynolds, J. G.; Burnham, A. K. (1997). Pyrolysis decomposition kinetics of cellulose-based materials by constant heating rate micropyrolysis. Energy Fuels, **11**, 88–97.
37. Becidan, M., Várhegyi, G., Hustad, J.E., and Skreiberg, Ø. (2007). Thermal decomposition of biomass wastes. A kinetic study, Ind. Eng. Chem. Res.**, 46**, 2428-2437.
38. Várhegyi, G., Bobály, B., Jakab, E., and Chen, H. (2011). Thermogravimetric Study of Biomass Pyrolysis Kinetics. A Distributed Activation Energy Model with Prediction Tests, Energy Fuels **25**, 24–32.
39. Di Blasi, C., Branca, C., Santoro, A., Hernandez, E. G. (2001).Pyrolytic behavior and products of some wood varieties, Comb. Flame **124**, 165–177.
40. Di Blasi, C., (2008). Modeling chemical and physical processes of wood and biomass pyrolysis, Progress in Energy and Combustion Science **34,** 47–90.
41. Bridgwater, A.V. (Editor), (2001). An Overview of Fast Pyrolysis, Vol. 2, Blackwell Science, London, UK,
42. Meier, D; Faix, O, (1999). State of the art of applied fast pyrolysis of lignocellulosic materials - a review, Biores. Technol. **68**, 71-77.
43. Bridgwater, A.V. (2012). Review of fast pyrolysis of biomass and product upgrading, Biomass and Bioenergy, **38**, 68–94.
44. Pictet A., and Sarasin, J. (1918). Sur la distillation de la cellulose et de l'amidon sous pression réduite, Helv. Chim. Acta, **1**, 87–96.
45. Épshtein, Ya. V., Golova, O. P., Durynina, L. I. (1959). Preparation of levoglucosan (β-D-1,6-anhydroglucopyranose) by the thermodegradation of cellulose in a stream of superheated steam under reduced pressure, Bull. Acad. Sci. USSR, Div. Chem.Sci. **8(6)**, 1089-1090.

46. Kwon, G.J., Kim, D-Y., Kimura, S., Kuga, S. (2007). Rapid-cooling, continuous-feed pyrolyzer for biomass processing. Preparation of levoglucosan from cellulose and starch, J. Anal. Appl. Pyrolysis **80**, 1–5.
47. Mamleev, V., Bourbigot, S., Le Bras, M., and Yvon, J. (2009). The facts and hypotheses relating to the phenomenological model of cellulose pyrolysis. Interdependence of the steps, J. Anal. Appl. Pyrolysis, **84(1)**, 1-17.
48. Várhegyi, G., Antal, M.J., Jr., Székely, T., Till, F., Jakab, E., (1988). Simultaneous Thermogravimetric-Mass Spectrometric Studies of the Thermal Decomposition of Biopolymers. 1. Avicel Cellulose in the Presence and Absence of Catalysts, Energy & Fuels **2**, 267-272.
49. Basch, A., Lewin, M. (1973). The influence of fine structure on the pyrolysis of cellulose. I. Vacuum pyrolysis, *J. Polym. Sci.* **11**, 3071-3093.
50. Rodrig, H., Basch, A., Lewin, M, (1975). Crosslinking and pyrolytic behavior of natural and man-made cellulosic fibers. J. Polym. Sci., Part A-Polym. Chem. **13(8)**, 1921-1932.
51. Basch, A., Lewin, M. (1975). Effect of orientation upon annealing of cellulose. J. Polym. Sci., Part C-Polym. Lett, **13(8)**, 493-499.
52. Golova, O. P., Merlis, N. M., Volodina, Z. V. (1958). Preparation of 1, 6-anhydroglucofuranose in thermal decomposition of cellulose under vacuum, Bull. Acad. Sci. USSR, Div. Chem.Sci. **7(9)**, 1093.
53. Faix, O., Fortmann, I., Bremer, J., and Meier, D. (1991). Thermal-degradation products of wood - gas-chromatographic separation and mass-spectrometric characterization of polysaccharide derived products. Holz Als Roh-Und Werkstoff **49**, 213-219.
54. Faix, O., Meier, D., and Fortmann, I. (1990) Thermal-degradation products of wood - gas-chromatographic separation and mass-spectrometric characterization of monomeric lignin derived products, Holz Als Roh-Und Werkstoff, **48**, 281-285.
55. Faix, O., Fortmann, I., Bremer, J., and Meier, D. (1991). Thermal-degradation products of wood - a collection of electron-impact (ei) mass- spectra of polysaccharide derived products, Holz Als Roh-Und Werkstoff , **49**, 299-304.
56. Faix, O., Meier, D., and Fortmann, I. (1990). Thermal-degradation products of wood - a collection of electron-impact (ei) mass-spectra of monomeric lignin derived products, Holz Als Roh-Und Werkstoff, **48**, 351-354.
57. Furneaux, R.H., Mason, J.M., Miller, I.J. (1988). A novel hydroxylactone from the Lewis acid catalysed pyrolysis of cellulose, J. Chem. Soc. Perkin Trans. **1**, 49–51.
58. Fabbri, D., Torri, C., Mancini, I. (2007). Pyrolysis of cellulose catalysed by nanopowder metal oxides: production and characterisation of a chiral hydroxylactone and its role as building block, Green Chem. **9**, 1374–1379.
59. Kelly, J., Mackey, M., Helleur, R.J. (1991). Quantitative-analysis of saccharides in wood pulps by quartz-tube pulse pyrolysis-polar phase gas-chromatography, J. Anal. Appl. Pyrolysis **19**, 105–117.
60. Helleur, R.J. (1987). Characterization of the saccharide composition of heteropolysaccharides by pyrolysis-capillary gas chromatography-mass spectrometry, J. Anal. Appl. Pyrolysis **11**, 297-311.
61. Torri, C., Adamiano, A., Fabbri, D., Lindfors, C., Monti, A., Oasmaa, A., (2010) Comparative analysis of pyrolysate from herbaceous and woody energy crops by Py-GC

with atomic emission and mass spectrometric detection J. Anal. Appl. Pyrolysis, **88(2)**, 175-180.
62. Pouwels, A.D., Tom, A., Eijkel, G.B., Boon, J.J. (1987). Characterization of beech wood and its holocellulose and xylan fractions by pyrolysis-gas chromatography-mass spectrometry J. Anal. Appl. Pyrolysis, **11**, 417-436.
63. Faix, O., Meier, D., and Grobe, I. (1987) Studies on isolated lignins and lignins in woody materials by pyrolysis-gas chromatography-mass spectrometry and off-line pyrolysis-gas chromatography with flame ionization detection J. Anal. Appl. Pyrolysis **11,** 403-416.
64. Genuit, W., Boon, J.J., Faix, O. (1987). Characterization of beech milled wood lignin by pyrolysis-gas chromatography photoionization mass-spectrometry. Anal. Chem. **59**, 508-513.
65. Del Rio, J.C., Rencoret, J., Prinsen, P., Martinez, A.T., Ralph, J., Gutierrez, A. (2012). Structural Characterization of Wheat Straw Lignin as Revealed by Analytical Pyrolysis, 2D-NMR, and Reductive Cleavage Methods J. Agr. Food Chem. **60,** 5922-5935.
66. Evans, R.J., Milne, T.A., and Soltys, M.N. (1986). Direct mass spectrometric studies of the pyrolysis of carbonaceous fuels. III. Primary pyrolysis of lignin. J. Anal. Appl. Pyrolysis. **9**, 207-236.
67. Pankaj K. Kanaujia, Y.K. Sharma, U.C. Agrawal, M.O. Garg, (2013). Analytical approaches to characterizing pyrolysis oil from biomass, Trends in Analytical Chemistry, **42**, 125-136.
68. del Rio, J.C., Gutierrez, A. (2006). Chemical composition of abaca (Musa textilis) leaf fibers used for manufacturing of high quality paper pulps. J. Agr. Food Chem. **54**, 4600-4610.
69. Mészáros, E., Jakab, E., Gáspár, M., Réczey, K., and Várhegyi, G. (2009). Thermal behavior of corn fibers and corn fiber gums prepared in fiber processing to ethanol. **85**, 11-18.
70. Oasmaa, A., Meier, D. (2005). Norms and standards for fast pyrolysis liquids - 1. Round robin test. J. Anal. Appl. Pyrolysis **73**, 323-334.
71. Meier, D. van de Beld, B., Bridgwater, A.V., Elliott, D.C., Oasmaa, A., Preto, F. (2013). State-of-the-art of fast pyrolysis in IEA bioenergy member countries. Renewable & Sustainable Energy Reviews **20**, 619-641.
72. Antal, M.J., Jr., Gronli, M. (2003).The art, science, and technology of charcoal production, Industrial & Engineering Chemistry Research **42(8)**, 1619-1640.
73. Broido, A., and Nelson, M.A. (1975). Char yield on pyrolysis of cellulose. Comb. Flame **24**, 263-268.
74. Várhegyi, G., Jakab, E., Antal, M.J., Jr., (1994). Is the Broido-Shafizadeh Model for Cellulose Pyrolysis True? Energy & Fuels, **8**, 1345-1352.
75. Pakhomov, A.M. (1957). Free-radical mechanism of the thermodegradation of cellulose and formation of levoglucosan, Bull. Acad. Sci. USSR, Div. Chem. Sci. **6(12)** 1525-1527.
76. Van der Kaaden, A., Haverkamp, J., Boon, J.J., De Leeuw, J.W. (1983). Analytical pyrolysis of carbohydrates .1. chemical interpretation of matrix influences on pyrolysis-mass spectra of amylose using pyrolysis-gas chromatography-mass spectrometry. J. Anal. Appl. Pyrolysis **5**, 199-220.

77. Zhang, X., Weihong Yang, W., Dong, C. (2013). Levoglucosan formation mechanisms during cellulose pyrolysis. J. Anal. Appl. Pyrolysis, **104**, 19–27.
78. Richards, G.N. (1987). Glycolaldehyde from pyrolysis of cellulose, J. Anal. Appl. Pyrolysis **10(3)** 251-255.
79. Piskorz, J., Radlein, D., and Scott, D.S. (1986). On the mechanism of the rapid pyrolysis of cellulose, J. Anal. Appl. Pyrolysis, **9**, 121–137.
80. Arisz P.W., and Boon, J.J. (1993). Pyrolysis mechanisms of O-(2- hydroxyethyl)-celluloses. J. Anal. Appl. Pyrolysis, **25**, 371-385.
81. Ponder, G.R., Richards, G.N., Stevenson, T.T. (1992). Mechanisms of pyrolysis of polysaccharides .6. Influence of linkage position and orientation in pyrolysis of polysaccharides - a study of several glucans, J. Anal. Appl. Pyrolysis, **22(3)**, 217-229.
82. Faix, O; Schweers, W. (1975). Comparative investigations on polymer models of lignins (dhps) of different composition .7. Pyrolysis. Holzforschung **29**, 224-229.
83. Faix, O; Meier, D; Fortmann, I (1988) Pyrolysis-gas chromatography-mass spectrometry of 2 trimeric lignin model compounds with alkyl-aryl ether structure. J. Anal. Appl. Pyrolysis **14**, 135-148.
84. Britt, P.F., Buchanan, A.C., Cooney, M.J., Martineau, D.R,(2000). Flash vacuum pyrolysis of methoxy-substituted lignin model compounds J. Org. Chem. **65**, 1376-1389.
85. Britt, P.F., Buchanan, A.C., Thomas, K.B., Lee, S.K. (1995). Pyrolysis mechanisms of lignin - surface-immobilized model-compound investigation of acid-catalyzed and free-radical reaction pathways J. Anal. Appl. Pyrolysis **33**, 1-19
86. Buchanan, A.C., Britt, P.F., (2000). Investigations of restricted mass transport effects on hydrocarbon pyrolysis mechanisms through silica immobilization. J. Anal. Appl. Pyrolysis **54**, 127-151.
87. Britt, P.F., Buchanan, A.C., Malcolm, E.A. (2000). Impact of restricted mass transport on pyrolysis pathways for aryl ether containing lignin model compounds. Energy & Fuels **14**, 1314-1322.
88. Jakab, E., Faix, O., Till, F., Székely, T. (1995). Thermogravimetry mass-spectrometry study of 6 lignins within the scope of an international round-robin test. J. Anal. Appl. Pyrolysis **35**, 167-179.
89. Mu, W., Ben, H., Ragauskas, A., and Deng, Y. (2013). Lignin pyrolysis components and upgrading - Technology review. Bioenerg. Res. **6**, 1183-1204.
90. Mészáros, E., Jakab, E., Várhegyi, G. (2007). TG/MS, Py-GC/MS and THM-GC/MS study of the composition and thermal behavior of extractive components of Robinia pseudoacacia, J. Anal. Appl. Pyrolysis, **79**, 61-70.
91. Várhegyi, G., Antal, M.J., Jr., Székely, T., Till, F., Jakab, E., Szabó, P., (1988). Simultaneous Thermogravimetric-Mass Spectrometric Studies of the Thermal Decomposition of Biopolymers. 2. Sugar Cane Bagasse in the Presence and Absence of Cata1ysts, Energy & Fuels **2**, 273-217.
92. Várhegyi, G., Jakab, E., Till, F. and Székely, T.(1989). Thermogravimetric-Mass Spectrometric Characterization of the Thermal Decomposition of Sunflower Stem, Energy & Fuels **3**,755-760.

93. Nowakowski, D.J., Jones, J.M. (2008). Uncatalysed and potassium-catalysed pyrolysis of the cell-wall constituents of biomass and their model compounds, J. Anal. Appl. Pyrolysis, **83**, 12–25.
94. Hosoya, T., Kawamoto, H., Saka, S., (2007). Influence of inorganic matter on wood pyrolysis at gasification temperature, J. Wood Sci., **53**, 351-357.
95. Shimada, N., Kawamoto, H., Saka, S. (2008). Different action of alkali/alkaline earth metal chlorides on cellulose pyrolysis. J. Anal. Appl. Pyrolysis **81**, 80–87.
96. Kawamoto, H., Yamamoto, D., Saka, S. (2008). Influence of neutral inorganic chlorides on primary and secondary char formation from cellulose. J. Wood Sci. **54**, 242–246.
97. Sebestyén, Z., Jakab, E., May, Z., Sipos, B., and Réczey K. (2013) Thermal behavior of native, washed and steam exploded lignocellulosic biomass samples, J. Anal. Appl. Pyrolysis **101**, 61–71.
98. Sebestyén, Z., Lezsovits, F., Jakab, E., and Várhegyi, G. (2012). Correlation between heating values and thermogravimetric data of sewage sludge, herbaceous crops and wood samples. J. Therm. Anal. Calorim. **110**, 1501–1509.
99. Gomez, C.J., Mészáros, E., Jakab, E., Velo, E., and Puigjaner, L. (2007). Thermogravimetry/mass spectrometry study of woody residues and an herbaceous biomass crop using PCA techniques. J. Anal. Appl. Pyrolysis **80**, 416–426.
100. Worasuwannarak, N., Sonobe, T., and Tanthapanichakoon, W. (2007). Pyrolysis behaviors of rice straw, rice husk, and corncob by TG-MS technique. J. Anal. Appl. Pyrolysis **78**, 265-271.
101. Sebestyén, Z., May, Z., Réczey, K., and Jakab, E. (2011). The effect of alkaline pretreatment on the thermal decomposition of hemp, J. Therm. Anal. Calorim. **105**, 1061–1069.
102. Jakab, E., Faix, O., Till, F., and Székely, T. (1993). The effect of cations on the thermal decomposition of lignins, J. Anal. Appl. Pyrolysis, **25**, 185-194.
103. Jakab, E., Mészáros, E., Borsa, J. (2010). Effect of slight chemical modification on the pyrolysis behavior of cellulose fibers. J. Anal. Appl. Pyrolysis **87**, 117–123.
104. Stocker, M., Biofuels and Biomass-To-Liquid Fuels in the Biorefinery: (2008). Catalytic Conversion of Lignocellulosic Biomass using Porous Materials. Angew. Chem.-Int. Ed. **47**, 9200-9211.
105. Torri, C., Reinikainen, M., Lindfors, C., Fabbri, D., Oasmaa, A., and Kuoppala, E. (2010). Investigation on catalytic pyrolysis of pine sawdust: Catalyst screening by Py-GC-MIP-AED. J. Anal. Appl. Pyrolysis, **88**, 7-13.
106. Torri, C., Lesci, I. G., Fabbri, D. (2009). Analytical study on the production of a hydroxylactone from catalytic pyrolysis of carbohydrates with nanopowder aluminium titanate. , J. Anal. Appl. Pyrolysis, **84**, 25-30.
107. Dobele, G., Dizhbite, T., Rossinskaja, G., Telysheva, G., Meier, D., Radtke, S., Faix, O. (2003). Pre-treatment of biomass with phosphoric acid prior to fast pyrolysis - A promising method for obtaining 1,6-anhydrosaccharides in high yields J. Anal. Appl. Pyrolysis, **68-9**, 197-211.
108. Dobele, G., Rossinskaja, G., Dizhbite, T., Telysheva, G., Meier, D., Faix, O. (2005). Application of catalysts for obtaining 1,6-anhydrosaccharides from cellulose and wood by fast pyrolysis. J. Anal. Appl. Pyrolysis, **74**, 401-405.

109. Dobele, G., Jakab, E., Volperts, A., Sebestyén, Z., Zhurins, A., Telysheva, G. (2013). Formation of nanoporous carbon materials in conditions of thermocatalytic synthesis, J. Anal. Appl. Pyrolysis, **103**, 173-180.
110. Bourgeois, J., Guyonnet, R. (1988). Characterization and analysis of torrefied wood. Wood Sci Technol;22(2):143-155.
111. Prins, M.J., Ptasinski K.J., Janssen F.J.J.G. (2006). Torrefaction of wood: Part 1. Weight loss kinetics. J Anal Appl Pyrolysis **77(1)**, 28-34.
112. Prins, M.J., Ptasinski, K.J, Janssen, F.J.J.G. (2006). Torrefaction of wood: Part 2. Analysis of products. J Anal Appl Pyrolysis **77(1),** 35-40.
113. Tjeerdsma, B.F., Boonstra, M., Pizzi, A., Tekely, P., Militz,,H. (1998). Characterisation of thermally modified wood: molecular reasons for wood performance improvement. Holz als Roh und Werkstoff **56(3),** 149-153.
114. Van der Stelt, M.J.C., Gerhauser, H., Kiel, J.H.A., Ptasinski, K.J. (2011). Biomass upgrading by torrefaction for the production of biofuels: a review. Biomass Bioenergy **35(9),** 3748–3762.
115. Kim, Y-H., Lee, S-M., Lee, H-W., Jae-Won Lee, J-W. (2012). Physical and chemical characteristics of products from the torrefaction of yellow poplar (Liriodendron tulipifera). Biores. Technol. **116**, 120–125.
116. Boateng, A.A., Mullen, C.A. (2013). Fast pyrolysis of biomass thermally pretreated by torrefaction. . J Anal Appl Pyrolysis **100**, 95–102.
117. Chang, S., Zhao, Z., Zheng, A., He, F., Huang, Z., and Li, H. (2012). Characterization of Products from Torrefaction of Sprucewood and Bagasse in an Auger Reactor, Energy Fuels **26**, 7009−7017.
118. Park, J., Meng, J., Lim K.H., Rojasa, O.J., Park, S., (2013). Transformation of lignocellulosic biomass during torrefaction. J. Anal. Appl. Pyrolysis, **100**, 199–206
119. Tooyserkani, Z., Sokhansanj, S., Bi, X., Lim, J., Lau, A., Saddler, J., Kumar, L., Lam, P.S., Melin, S., (2013). Steam treatment of four softwood species and bark to produce torrefied wood. Appl. Energ. **103**, 514–521
120. Grinins, J., Andersons, B., Biziks, V., Andersone, I., Dobele, G. (2013). Analytical pyrolysis as an instrument to study the chemical transformations of hydrothermally modified wood. J. Anal. Appl. Pyrolysis, **103**, 36-41.
121. Karagoz, S., Bhaskar, T., Muto, A., Sakata, Y., and Uddin, M.A. (2004). Low-temperature hydrothermal treatment of biomass: Effect of reaction parameters on products and boiling point distributions. Energy & Fuels **18**, 234-241.